CHAPTER 1
INTRODUCTION

1.1 Background of Study

Natural gas is widely and commonly used as a source of fuel and is a vital component of the world's energy supply (Natural Gas Supply Association, 2004). Natural gas have both industrial (production of Ammonia in ASEAN Bintulu Fertilizer Sdn. Bhd.) and domestic (cooking, heating) applications.

It is colorless, odorless and regarded as one of the safest and cleanest source of fuel. Natural gas comprises of hydrocarbons, carbon dioxide, oxygen, nitrogen, hydrogen sulfide and traces of rare gases at times (Time for Change, 2007).

Methane	CH_4	70-90%
Ethane	C_2H_6	0-20%
Propane	C_3H_8	
Butane	C_4H_{10}	
Carbon Dioxide	CO_2	0-8%
Oxygen	O_2	0-0.2%
Nitrogen	N_2	0-5%
Hydrogen Sulphide	H_2S	0-5%
Rare Gases	Ar, He, Ne, Xe	Traces

Table 1: Composition of Natural Gas

(Source: Time for Change, 2007)

It is also a major source of electricity generation by using natural gas to power steam and gas turbines. Not only that, natural gas can also be used to produce pulp, paper, metals, stones, clays, chemicals, glasses and also to process certain food or to even treat waste materials (Abou-Arab, 1986)

When the fuels ignite, they generate energy by converting carbon to carbon dioxide and hydrogen to water vapor (Petroleum Newspapers of Alaska, 2009). Combustion of natural gas generally emits lower CO_2 content as compared to the combustion of other sources of fuel, such as oil and coal.

Pollutant	Natural Gas	Oil	Coal
Carbon Dioxide	117,000	164,000	208,000
Carbon Monoxide	40	33	208
Nitrogen Oxides	92	448	457
Sulfur Dioxide	1	1,122	2,591
Particulates	7	84	2,744
Mercury	0.000	0.007	0.016

Table 2: Fossil Fuel Emission Levels – Pounds per Billion Btu of Energy Input
(Source: EIA-Natural Gas Issues and Trends, 1998)

Years ago, natural gas was one of the gas sources that were 'ignored' as the cost for treating this gas was immensely high which thus made it costly to be sold in the market. But now as the demand for alternative fuel source is increasing rapidly, gas suppliers are turning to natural gas, treating them and making them saleable.

The technology for treating natural gas has been developed. Natural gas is now treated to remove impurities, such as carbon dioxide (CO_2), other particulates and components to meet the plant's requirements, or simply the customer's specifications.

CO_2 contributes the most percentage to the cause of global warming. Global warming happens by the emission of greenhouse gases, which are carbon dioxide (CO_2) 72%, Methane (CH_4) 18% and Nitrous Oxide (NOx) 9% (Time for Change, 2007). By removing carbon dioxide (CO_2) from natural gas, the release of carbon dioxide to the atmosphere can hence be lowered.

Though natural gas may be regarded as one of the cleanest source of fuel as compared to the other sources, the emission of CO_2 during the combustion of natural gas does substantially contribute to global warming.

Carbon dioxide (CO_2) removal can alleviate the greenhouse effect problem by reducing the net CO_2 emission from industrial waste gases, which would otherwise be vented into the atmosphere (Aroonwilas, 1996).

Besides that, by removing CO_2 from natural gas, this can also help to improve the heating value of the gas apart from meeting customer's specification and for successful liquefaction process in Liquefied Natural Gas (LNG) processes (Ebenezer, 2005).

There are works where researches injected high concentration of carbon dioxide (CO_2) in natural gas into absorption column filled with random packing for stripping / removal purposes with another solvent such as aqueous monoethanolamine (MEA) solution. For example, works done by Liu et al (2006). Most of these works are experimental forms (experiments / labs) whereby results will be collected, analyzed and justified.

The Computational Fluid Dynamics (CFD) modeling is basically the modeling of the hydrodynamic behavior of the gas and liquid contact. It is well known that the most accurate methods of separation processes are based on the continuous mechanics consideration, and thus the method of Computational Fluid Dynamics (CFD) represents a promising application (Mahr and Mewes, 2007).

In the recent years, there have been significant academic and industrial efforts to exploit Computational Fluid Dyanmics (CFD) for the design, scale-up and optimal operation of various chemical processes equipment (Nikou et al., 2008).

1.2 Problem Statement

The journals regarding Computational Fluid Dynamics (CFD) modeling for random packings are limited. Many research and findings have been conducted by various people in the world regarding the removal of high concentration of carbon dioxide (CO_2) from natural gas using absorption method through experimental / lab work. But very little work has been done regarding the Computational Fluid Dynamics (CFD) modeling for hydrodynamics behavior for the gas and liquid contact.

Natural gas which contains high content of carbon dioxide will emit carbon dioxide and water into the atmosphere when combusted with air. The carbon dioxide released contributes to global warming problems. Thus, the high content of carbon dioxide in natural gas must be removed to help alleviate global warming issues.

1.3 Objectives

The major objectives of this project are as follows:

- To simulate hydrodynamic model and mass transfer for high carbon dioxide (CO_2) content in natural gas in absorption column with random packing
- To determine the effect of different column height in absorption process
- To determine the effect of different gas velocities in absorption process
- To determine the grid sensitivity analysis for the GAMBIT mesh

1.4 Scope of Study

The study is concerned with the usage of random packing to promote better absorption rate between the natural gas with high CO_2 concentration and the solvent, monoethanolamine (MEA) solution. The purpose of the random packing is to provide better and larger surface area contact between the natural gas and the solvent. Simulation software like FLUENT will be used to determine the multiphase flow within the random packing.

The same simulation will be repeated for different column heights to determine the effect of different absorption column heights and different gas velocities on the absorption process. The grid sensitivity analysis would then be conducted for the absorption column mesh.

1.5 Relevancy of the Project

Very little work / research has been done regarding the hydrodynamic behavior and mass transfer for the removal of CO_2 from natural gas using absorption method in random packing. Apart from meeting the pipeline's and customer's specification, another solid reason to remove CO_2 from natural gas is to reduce the contribution of greenhouse gases to the world's global warming issue. Not only that, the removal of CO_2 can improve the heating value of the fuel.

1.6 Feasibility of the Project within the Scope and Time Frame

The first four months will cover mostly literature review on absorption columns, random packing, Computational Fluid Dynamics (CFD) and FLUENT software. After the literature review, the author will simulate the hydrodynamic and mass transfer of gas and liquid using FLUENT simulation. Once done, the simulation will be repeated for different column heights and different gas velocities. Finally, the grid sensitivity analysis will be conducted for the mesh.

CHAPTER 2
THEORY AND LITERATURE REVIEW

2.1 Theory

2.1.1 The Reaction Mechanism of CO_2 Absorption by Aqueous Monoethanolamine (MEA) Solution

According to Danckwerts (1979) and Astarita et al. (1964), when CO_2 is absorbed and reacts with aqueous MEA, three overall reactions takes place at the condition of carbonation ratio or CO_2 loading less than 0.5 mol of CO_2 per mole of MEA.

2.1.1.1 First Reaction

$$CO_{2,g} \longrightarrow CO_{2,L} + H_A$$

This equation represents the physical absorption of CO_2 by water and H_A is the accompanied heat of solution.

2.1.1.2 Second Reaction

$$CO_{2,L} + 2HOCH_2CH_2{}^{-}NH_2 \xrightarrow{k_2} HOCH_2CH_2{}^{-}NHCOO^{-} + HOCH_2CH_2{}^{-}NH_3{}^{+} + H_R$$

The second reaction takes place in two steps:

$$CO_{2,L} + HOCH_2CH_2{}^{-}NH_2{}^{-} \longrightarrow HOCH_2CH_2{}^{-}NHCOO^{-} + H^{+}$$

(1)

$$HOCH_2CH_2\text{-}NH_2 + H^{+} \longrightarrow HOCH_2CH_2{}^{-}NH_3{}^{+}$$

(2)

Reaction (1) is considered as second order and is the rate controlling step. Reaction (2) is a proton transfer reaction and is virtually instantaneous.

2.1.1.3 Third Reaction

$$CO_{2,L} + HOCH_2CH_2{}^{-}NHCOO^{-} + 2H_2O \longrightarrow HOCH_2CH_2{}^{-}NH_3{}^{+} + 2HCO_3{}^{-}$$

According to Sada et al. (1976), at very short times of the liquid-gas encountered in industrial absorbers, this reaction can be neglected and only the second reaction affects the absorption rate of CO_2.

Thus, the absorption of CO2 in MEA solutions can be regarded as gas absorption accompanied by an irreversible second-order reaction with a stoichiometric coefficient of 2 (Liu et al., 2006).

The overall reaction can be represented by the second reaction found in 2.1.1.2. The reaction rate can be expressed by:

$R_c = k_2[CO_2][MEA]$

2.1.2 The k-ε Equation in FLUENT

In FLUENT software simulation, the k-ε equation is selected under the viscous model section. The standard k-ε equation is chosen as the packing itself is considered to be in turbular flow. The standard k-ε equation consists of turbulent kinetic energy (k) and the turbulent dissipation rate (ε).

The k-ε equation has two equation models in which the solution of two separate transport equation allows the turbulent velocity and length scales to be independently determined. The assumption made when using this model is that the flow is fully turbulent and the effects of molecular viscosity are negligible.

2.1.2.1 The Turbulent Kinetic Energy (k) Equation

$$\nabla \cdot (\rho h \mathbf{u} k) - \nabla \cdot \left[h \left(\mu + \frac{\mu_t}{\sigma_k} \right) \nabla k \right] = h\, \mu_{\text{eff}}\ \nabla \mathbf{u} \cdot ((\nabla \mathbf{u} + (\nabla \mathbf{u})^{\mathrm{T}}) - \frac{2}{3}\ \nabla \cdot \mathbf{u}\mathbf{I}) - \rho h \varepsilon$$

2.1.2.2 The Turbulent Dissipation Rate (ε) Equation

$$\nabla \cdot (\rho h \mathbf{u} \mathcal{E}) - \nabla \cdot \left[h \left(\mu + \frac{\mu_t}{\sigma_{\mathcal{E}}} \right) \nabla \mathcal{E} \right] = c_1 h\, \mu_{\text{eff}}\ \nabla \cdot \mathbf{u}\ ((\nabla \cdot \mathbf{u} + (\nabla \cdot \mathbf{u})^{\mathrm{T}}) - \frac{2}{3}\ \nabla \cdot\ \mathbf{u}\mathbf{I})\ \frac{\mathcal{E}}{k}$$

$$-\ (c_2 \rho h \frac{\mathcal{E}^2}{k})$$

where the parameters specified in FLUENT software are chosen to be:

$C_\mu = 0.09$, $c_1 = 1.44$, $c_2 = 1.92$, $\sigma_k = 1.0$, $\sigma_\varepsilon = 1.3$

2.1.3 The Accompanied CFD Equations

2.1.3.1 The Continuity Equation

When fluid is in motion, it must move in a way that mass is conserved (Princeton University, 2011). The rough idea of the principality of conservation is that the total amount of conserved quantity inside any region can only be changed by the amount that passes in or out of the region through the boundary. Simply put, a conserved quantity cannot increase or decrease, it can only move from place to place.

The continuity equation used in this research is:

$$\nabla \cdot (\rho h \mathbf{u}) = M$$

where ρ = liquid density

h = volume fraction of liquid phase based on pore space

$\mathbf{u}$ = interstitial velocity vector

M = source term of the continuity equation due to the chemical absorption of CO_2 from gas phase which is equal to the quantity of CO_2 absorbed by the aqueous solution per unit volume and unit time

2.1.3.2 The Momentum Equation

The momentum equation is a statement of Newton's second law and relates the sum of the forces acting on an element of fluid to its acceleration or rate of change of momentum. Newton's 2nd Law says that the rate of change of momentum of a body is equal to the resultant force acting on the body and takes place in the direction of the force (Cartage, 2009).

The momentum equation:

$$\nabla \cdot (\rho h \mathbf{u}\mathbf{u}) - \nabla \cdot \left(h\, \mu_{eff} \left[\left(\nabla \mathbf{u} + (\nabla \mathbf{u})^T - \frac{2}{3} \nabla \cdot \mathbf{u} I\right)\right]\right) = -h \nabla p + \mathbf{F}_{LG} + h\, (\mathbf{F}_{LS} + \rho \mathbf{g})$$

where μ_{eff} = effective viscosity

F_{LG} = interface drag force between gas phase and liquid phase

F_{LS} = flow resistance created by random packing (body force)

2.2 Literature Review

2.2.1 Removal of Carbon Dioxide from Natural Gas

As stated in Introduction, carbon dioxide (CO_2) is one of the major contributors to global warming. Global warming occurs when green house gases are released into the atmosphere. Carbon dioxide itself contributes 72% alone to global warming. If this problem is not tackled from now onwards, the repair and damage may be irreversible in the coming future.

Thus, by removing the amount of carbon dioxide in natural gas, the global warming problem can be alleviated step by step. Many ways and methods have been proposed to reduce global warming issues such as reduce the usage of air conditioning and heater (Environment About, 2011). One of the many ways includes removing CO_2 content from natural gas. CO_2 gas removal from natural gas becomes essential as this method helps alleviates the global warming problem.

Gas sweetening is a process where CO_2 is removed from the fuel (Xiao et al., 2008). The removal of CO_2 as stated by Bhide et al. (1998) is to

- Increase fuel heating value
- Decrease the volume of gas to be transported within pipelines
- Reduce pipeline corrosion within the gas networking system
- Prevent atmospheric pollution

With existing technologies, CO_2 removal can be achieved by several separation techniques including absorption into liquid solvents, adsorption on solids, permeating through membranes, and chemical conversion (Faisal M. Khan and Dr Tariq Mahmud, 2008). For CO_2 capture from large volume gas streams, the absorption into liquid solvents is the most feasible process approach (Kohl and Nielsen, 1997).

Conventionally, CO_2 absorption takes place in packed or tray columns that allow direct contact between gas streams containing CO_2 and the liquid solvent. Removal performance of the absorption process can be determined by the degrees of gas-liquid contact provided by column internals (Faisal M. Khan and Dr Tariq Mahmud, 2008).

2.2.2 Absorption Process

Absorption is a process by which a substance incorporated in one state is transferred into another substance of a different state (Citizendium, 2010). For example, absorption process takes place when gas is absorbed into liquid or liquid is absorbed into solid. Commonly practiced in industries, absorption process is most commonly used for the separation or the purification of a gas mixture with a solvent.

2.2.2.1 Physical Absorption

According to Ebenezer (2005), physical absorption processes use organic solvents to physically absorb acid gas components rather than react chemically. Physical absorption of a gas mixture in a liquid solvent involves the mass transfer that occurs at the interface between the gas and the liquid and the rate at which the gas diffuses into the liquid (Citizendium, 2010).

Removal of CO_2 by physical absorption processes are based on the mass transfer of CO_2 into the monoethanolamine (MEA) solvents. Solvents that are not chemically reactive to absorb solute are generally used in physical absorption where no chemical reaction takes place.

2.2.2.2 Chemical Absorption

According to Citizendium (2010), chemical absorption, also known as reaction absorption, involves a chemical reaction between the substance being absorbed and the absorbing medium. There are cases where chemical absorption occurs in combination with physical absorption. Chemical absorption depends upon the stoichiometry of the reaction and the concentration of the reactants.

Removal of CO_2 by chemical absorption processes are based on the solubility and the reaction of CO_2 with the monoethanolamine (MEA) solvents. Solvents that are chemically reactive to absorb solute are generally used in chemical absorption where chemical reaction takes place.

2.2.3 Packed Columns

In the chemical industry, packed columns have been widely used in purification and separation processes involving gas and liquid contact. According to Liu et al. (2006), packed columns are usually used in distillation and absorption processes due to its high efficiency, high capacity and low pressure drop. Packed columns are generally divided into 2 types, structured packing or random packing.

2.2.3.1 Random Packing

Random packing, like structured packing, is commonly used in refinery, gas processing, chemical and environmental process industries (Dohntec Ceramics Ltd, 2010). Despite the success of applying structured packing in the recent years, random packed columns are still commonly used in separation processes (Gualito et al., 1997; Spiegel and Meier, 2003).

Random packing has high density and excellent heat and acid resistance. Not only that, random packing such as Berl Saddles, Ceramic Pall Rings and Raschig Rings can withstand the corrosion of various inorganic acids, organic acids and organic solvents except for hydrofluoric acid (Dohntec Ceramics Ltd, 2010).

In this research, the absorption column is filled with random packing to simulate the flow, behavior and characteristics between the incoming natural gas with carbon dioxide (CO_2) and the solvent which is the monoethanolamine (MEA) solution. Packed beds formed by dumping bulk random packing elements of consistent shape and size will provide the consistent surface and voidage (volume of voids in sample) characteristics necessary for predictable mass transfer (Hat International, 2010).

There are various types of random packing, such as Berl Saddles, Ceramic Pall Rings and Raschig Rings. In this research, the author would be concentrating on the usage of Berl Saddles as the main random packing choice.

Berl Saddle is a first generation of random packing. It has an opening packing shaped like a saddle without inside and outside. It performs better as compared to Raschig Rings in the aspects of even fluid distribution and low resistance. Berl Saddles create

lower pressure against the inner wall of the column than ring packing (Dohntec Ceramic Ltd, 2010).

Berl Saddles relatively have larger specific surface area as compared to Raschig Rings. The common sizes for Berl Saddles random packing is from 10mm to 90mm and these Berl Saddles are usually made from ceramics, metals, polypropylene, plastic and other materials.

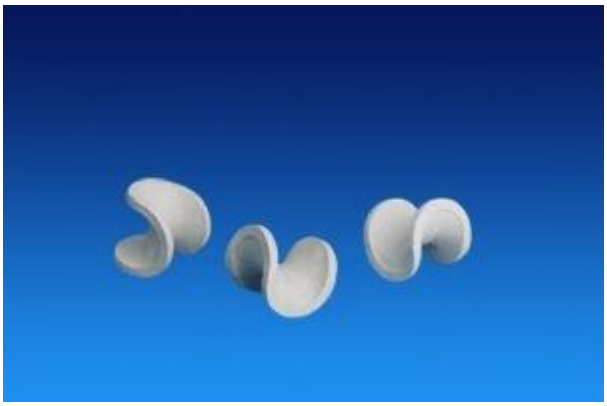

Figure 1: Berl Saddles Random Packing

(Source: Dohntec Ceramic Ltd, 2010)

2.2.4 Hydrodynamic Analogy and Computational Fluid Dynamics (CFD)

In the present paper, the hydrodynamic analogy idea is applied to rigorous modeling in columns equipped with random packing. The hydrodynamic analogy is the opportunity to employ the rigorous equations of continuum mechanism even for cases in which the real phase boundaries cannot be localized (Shilkin and Kenig, 2005).

To simulate the hydrodynamic behavior of the gas and liquid contact, it is required to understand Computational Fluid Dynamics (CFD). Computational Fluid Dynamics (CFD) is part of computational mechanics, which is part of simulation techniques. Simulation is used by various people from various occupations like engineers and scientist to forecast or even reconstruct the behavior of an engineering product or even a matter under assumed / measured boundary conditions.

Simulation like Computational Fluid Dynamics (CFD) is able to give insights to the users regarding the performances of certain equipments or even products.

Experiments, contradictorily to simulations, are costly. Simulation requires a sophisticated computer to run the software for simulation purposes, whereas experiments require raw materials and certain materials which may take up a very long time to get hold on.

The k-ε equation is used and the pressure based coupled solver is chosen as the simulation involves multiphase conditions and incompressible flows.

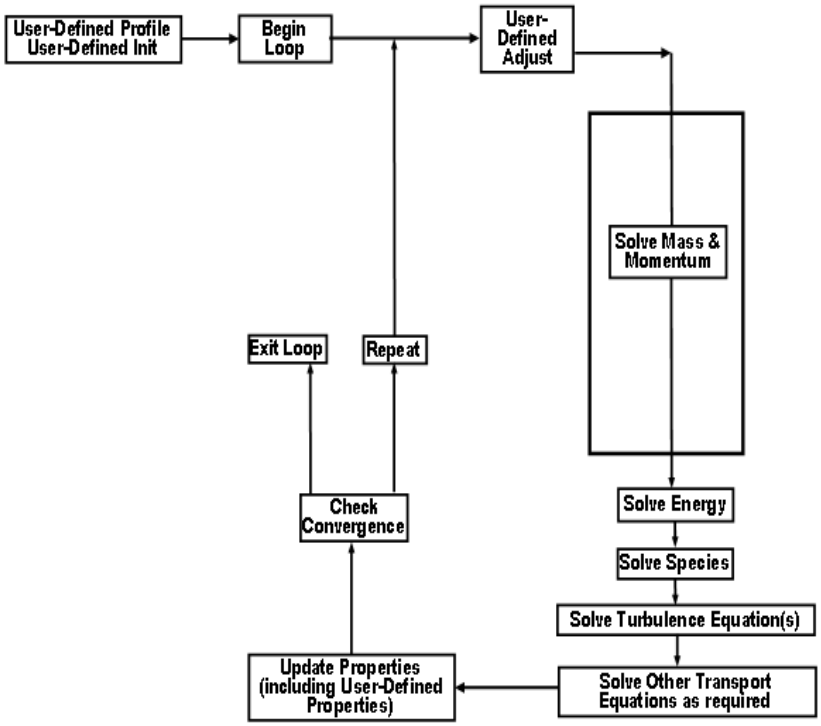

Figure 2: Solution Procedure for Pressure-Based Coupled Solver

2.2.5 User Defined Function (UDF)

A user-defined function, UDF, is a function program that can be dynamically loaded with the FLUENT solver to enhance the standard features of the code. UDFs can be used to define boundary conditions, material properties, source terms for flow regime, specify customized model parameters, initialize a solution or even to enhance post-processing.

UDFs are written in C programming language and the source code file is saved with a .c extension. UDFs are defined using DEFINE macros provided by Fluent Inc and must contain the udf.h file inclusion directive. Source files containing UDFs can either be interpreted or compiled in FLUENT (Fluent Inc, 2006).

In this simulation, interpreted UDFs are used. For interpreted UDFs, source files are interpreted and loaded directly at runtime in a single-step process. After interpreted, UDFs will become visible and can be selected in FLUENT graphics panel and can hooked to a solver by choosing the function name in the appropriate panel.

In summary, UDFs:

- are written in the C programming language
- must have an include statement for the udf.h file
- must be defined using DEFINE macros supplied by Fluent Inc
- utilize predefined macros and functions supplied by Fluent Inc. to access FLUENT solver data and perform other tasks
- are executed as interpreted or compiled functions
- are hooked to a FLUENT solver using a graphical user interface panel

In this simulation, 9 different UDF files are used to define and customize:

- the porousity for Berl Saddles
- the mass transfer between CO_2 and MEA solvent
- the drag law between the upcoming gas flow and the down coming liquid flow
- the volume fraction and species of gas and liquid throughout the column
- the outlet flow rate, inertial resistance and viscous resistance for gas and liquid

2.2.6 Overview of Absorption Column with Random Packing

An absorber of 0.1m inner diameter packed with ½" (12.7mm) ceramic Berl Saddles up to column height of 6.55m is used for this research's simulation. The absorber is operated in countercurrent mode and near ambient conditions.

The monoethanolamine (MEA) solvent will be injected into the absorber from the top inlet. Then the natural gas containing high concentration of CO_2 is passed into the bottom of the absorber and flows upwards against a countercurrent stream of solvent flowing down. In this simulation, the natural gas with CO_2 is replaced with air with CO_2.

The gas and the liquid will come into contact, forcibly by the random packing which demands the gas and liquid to take complicated paths, thus having larger surface area of contact enhancing the absorption process.

There will be two outlets from the absorption column, whereby the outlet at the top will be the outlet for the air stripped out from the high concentration of CO_2. The bottom outlet would be the outlet for the rich solvent for the solvent contains high concentration of CO_2.

The FLUENT software will be used to simulate the flow of the natural gas and the solvent within the random packing. This simulation will help the users to understand better the hydrodynamic behavior and mass transfer of both the gas and liquid. Not only that, the users will be able to optimize the removal of CO_2 based on this software in the future.

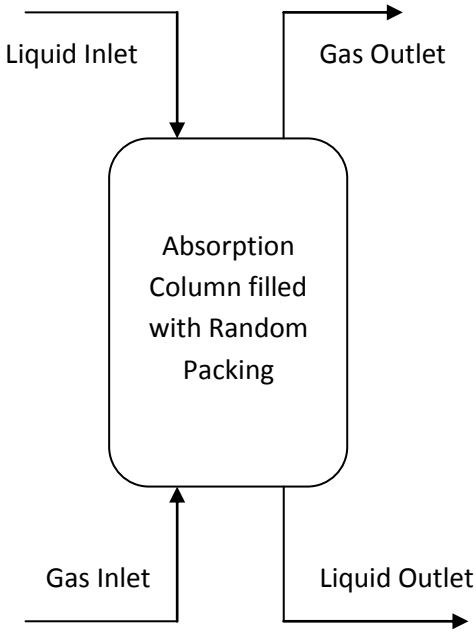

Figure 3: Absorption Column with Inlets and Outlets

The assumptions made based on this simulation are:

1. The gas absorption operation within the column is steady, and the liquid is incompressible, which means that the liquid density does not vary with the liquid temperature and concentration.

2. Only CO_2 from the gas phase component is absorbed into the aqueous MEA solvent, and the solvent does not transfer to the gas phase.

3. The flow simulation is axis-symmetric.

The boundary conditions are:

(1) At the inlet, the boundary condition for liquid phase is set to be $\mathbf{u} = \mathbf{u}_{inlet}$, $v_{inlet} = 0$,

$T = T_{inlet}$, $k_{inlet} = 0.0003u_{inlet}^2$, $\varepsilon_{inlet} = 0.09\ (k_{inlet}^{1.5}/d_H)$ (Khalil et al., 1975). The liquid superficial velocity is calculated using $L = \rho h \gamma |\mathbf{u}|$.

where

ρ = liquid density (kg/m^3)

h = volume fraction of liquid phase based on pore space (dimensionless)

γ = porosity of random packing bed along radial direction (dimensionless)

$|\mathbf{u}|$ = liquid interstitial velocity (m/s)

(2) At the outlet, the liquid flow at the bottom exit of the column is considered to be close to the fully developed condition, so the 'outflow' boundary condition of zero normal gradient for all flow variables except pressure is chosen under the platform of the FLUENT software. For gas flow, the boundary condition for gas phase is set to be $\mathbf{u} = \mathbf{u}_{inlet}$, $v_{inlet} = 0$, $T = T_{inlet}$, $k_{inlet} = 0.0003u_{inlet}^2$, $\varepsilon_{inlet} = 0.09\ (k_{inlet}^{1.5}/d_H)$ (Khalil et al., 1975). The gas superficial velocity is calculated using $L = \rho h \gamma |\mathbf{u}|$.

where

ρ = gas density (kg/m^3)

h = volume fraction of gas phase based on pore space (dimensionless)

γ = porosity of random packing bed along radial direction (dimensionless)

$|\mathbf{u}|$ = gas interstitial velocity (m/s)

(3) For axis, it is assumed that all variables Φ are axially symmetrical, thus $\frac{\partial \Phi}{\partial r} = 0$ at $r = 0$.

(4) The no slip condition is applied to the walls of the column, and the flow behavior in the near wall region is approximated by using the 'standard wall functions'. The zero flux condition is applied for other variables.

CHAPTER 3
METHODOLOGY

3.1 Research Methodology

3.1.1 Preparation of Absorption Column Meshing for Simulation using GAMBIT Software

For this research, the grid arrangement of the column of 6.55m height and 0.05m radius is 1310 nodes uniformly distributed along the column height and 80 nodes non-uniformly distributed along the radial direction with high grid resolution at the near wall region. For the 80 nodes non-uniformly distributed along the radial direction, the exponent type is used with a ratio of 0.29. The total quadrilateral cells are 104 800.

The top and bottom of the column is specified under the velocity inlet type; meanwhile the wall of the column is specified under the wall type. Since the drawing of the column is half of the actual size (0.1m), the lower line of the drawing will be specified under the axis type for the column is an axisymmetric geometry. The continuum type in the meshing is specified as fluid, as there will be interaction between gas and liquid phase.

The meshing is done in 2D face. Once the meshing is completed, the meshing will be exported as mesh into FLUENT software for simulation.

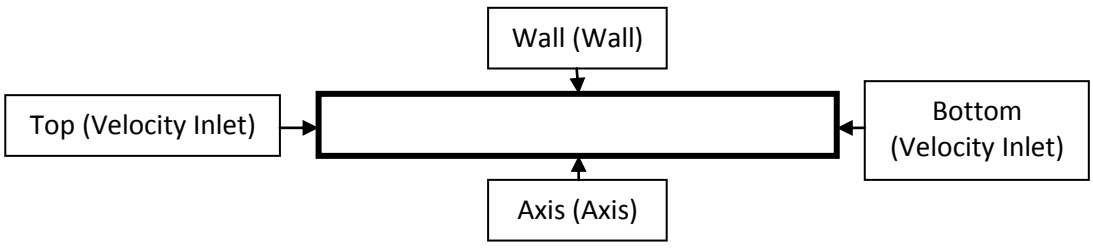

Figure 4: Boundary Conditions Arrangement

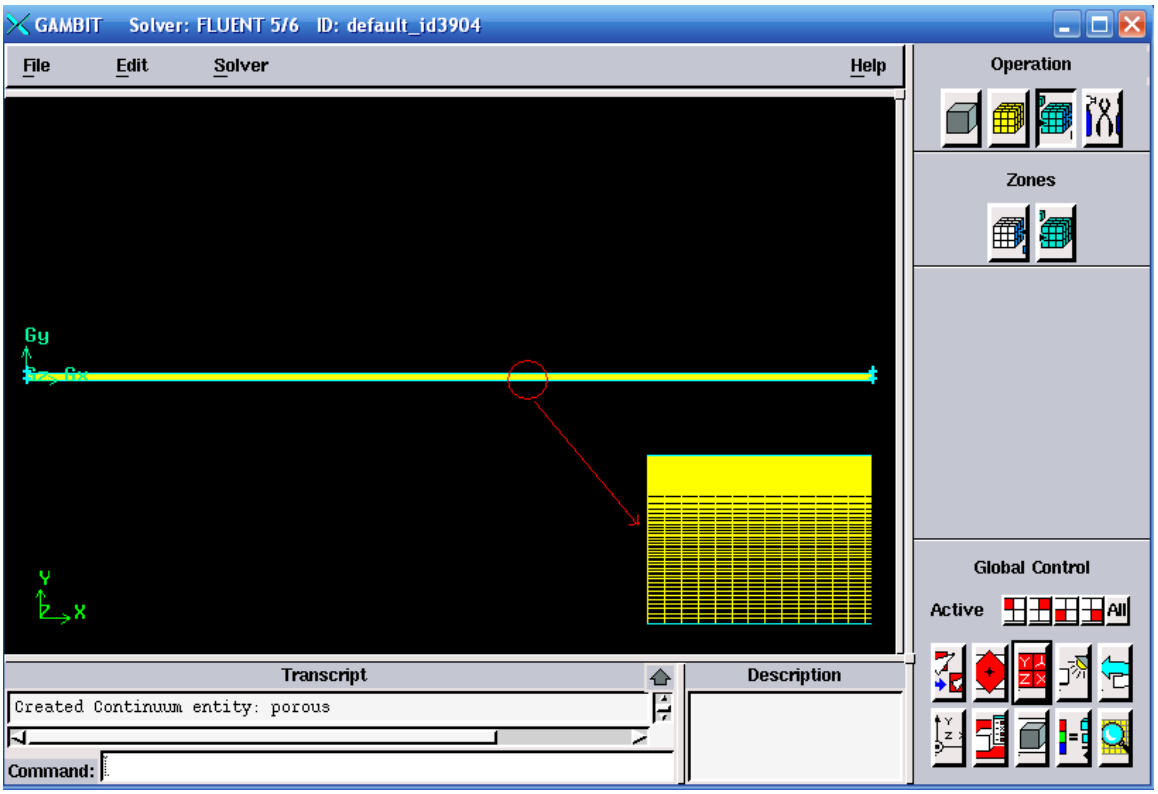

Figure 5: Drawing of Column Meshing

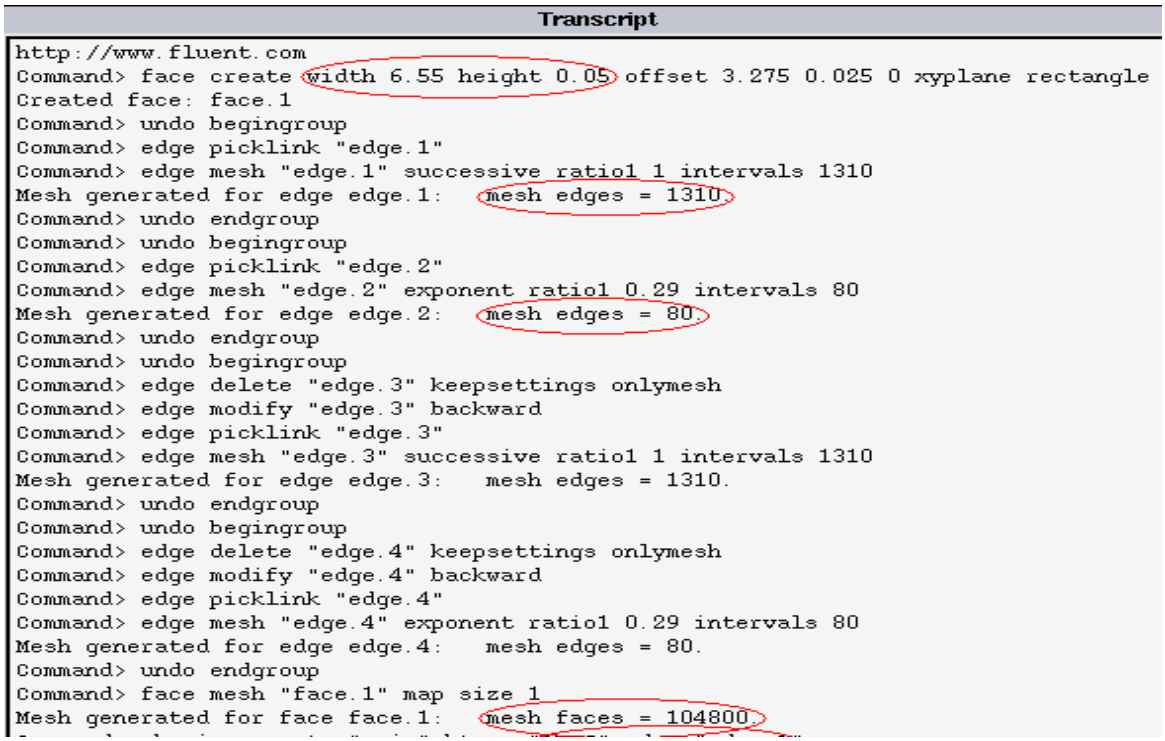

Figure 6: Mesh Face of 104 800 Quadrilateral Cells are Generated

```
Command> physics create "axis" btype "AXIS" edge "edge.1"
Created Boundary entity: axis
Command> physics create "outlet" btype "VELOCITY_INLET" edge "edge.2"
Created Boundary entity: outlet
Command> physics modify "axis" btype "WALL" label "wall" edge "edge.3"
Command> physics create "inlet" btype "VELOCITY_INLET" edge "edge.4"
Created Boundary entity: inlet
Command> physics create "axis" btype "AXIS" edge "edge.1"
Created Boundary entity: axis
Command> physics create "porous" ctype "FLUID" face "face.1"
Created Continuum entity: porous
```

Figure 7: Boundary Conditions are labeled and Continuum Entity is specified

3.1.2 Simulation of Hydrodynamic Behavior and Mass Transfer using FLUENT Software

The mesh is exported from GAMBIT software into FLUENT software for simulation. The solver for the simulation is defined to be pressure based as the simulation involves multiphase components and incompressible flow. Axisymmetric space is chosen as the previous meshing was done with an axis boundary. Eulerian model is specified with 2 phase as the model solves momentum and continuity equation for each phase.

The viscous model of k-ε is specified, species transport is selected as this can help to model the mixing and the transport of chemical species by solving conservation equations describing convection, and diffusion sources for each component species. The materials are done specified, generally the mixture-template consisting of air and CO_2 and aqueous MEA solvent. Turbulent model is chosen as justified in appendix ii part (7).

The interaction between gas phase and liquid phase is set. The drag coefficient and mass transfer mechanism is set by hooking respective UDFs. The operating pressure is set at 101325 Pa, operating temperature of 288.16K with gravity of 9.81 m/s^2. The boundary condition for gas inlet and liquid inlet is then specified. The flowrate is calculated based on the $L = \rho h \gamma |\mathbf{u}|$ equation. The initial mass fraction of CO_2 species in air is set to be 0.2165.

Once done, a set of initial values are predicted to solve the simulation. The absolute convergence criterion is set to 0.001.

3.2 Project Activities

Throughout the whole 8 months of research, several targets have been set. There are no specific datelines for which most of these targets must be achieved. The main activities would be:

- Literature review on absorption process, random packing, Computational Fluid Dynamics (CFD), GAMBIT and FLUENT software
- Determining the type of modeling used
- Learning on how to use the GAMBIT and FLUENT software
- Simulation for the absorption process
- Repetition of simulation for different column heights, different gas velocities
- Conducting grid sensitivity analysis for mesh
- Collection of simulation results for analysis and justification
- Conclusion of the whole research

The first four months of the whole 8 months research duration will be used to cover the first 3 main activities. The remaining 4 months will be used to simulate the hydrodynamic behavior and mass transfer for the gas and liquid phase. Simulations will be repeated for different column heights, different gas velocities and grid sensitivity analysis. The results will be analyzed and justified.

3.3 Key Milestones

No.	Activities	Due (Week)	Status
1.	Selection of Final Year Project Topic	2	Completed
2.	Literature Review on Removal of CO_2, Absorption Process, Random Packing, CFD Analogy	8	Completed
3.	Seminar	8	Completed
4.	GAMBIT and FLUENT Software Training	12	Completed
5.	Submission of Interim Report	13	Completed
6.	Oral Presentation	13	Completed

Table 3: Milestones for Final Year Project I

No.	Activities	Due (Week)	Status
1.	Preparation of Absorption Column Meshing	2	Completed
2.	Simulation of Hydrodynamic Behavior and Mass Transfer for Gas and Liquid Phase	6	Completed
3.	Submission of Progress Report	8	Completed
4.	Simulation of Hydrodynamic Behavior and Mass Transfer based on Different Column Heights	10	Completed
5.	Simulation of Hydrodynamic Behavior and Mass Transfer based on Different Gas Velocities	10	Completed
6.	Grid Sensitivity Analysis	10	Completed
7.	Pre-SEDEX	11	Completed
8.	Submission of Dissertation (Soft Bound)	13	Completed
9.	Submission of Technical Paper	After Week 14	
10.	Oral Presentation	After Week 14	
11.	Submission of Dissertation (Hard Bound)	After Week 14	

Table 4: Milestones for Final Year Project II

3.4 Gantt Chart

The Gantt Chart for the overall course will be attached accordingly in Appendix 1.

The Gantt Chart for this research will be attached accordingly in Appendix 1.

3.5 Tool (e.g. Equipment, Hardware, etc.) Required

The software that is needed for this research would be the GAMBIT and FLUENT software. The GAMBIT software will be used for drawing and meshing and the FLUENT software will be used to simulate the flow within the column.

CHAPTER 4
RESULTS AND DISCUSSION

4.1 Results for Part I: To Determine Hydrodynamic Behavior and Mass Transfer of Gas and Liquid Phase

4.1.1 FLUENT Simulation

The simulation is simulated using FLUENT software and is solved by using 2D version. In this simulation, the author simulates the hydrodynamic behavior and the mass transfer between gas and liquid contact. The momentum equation used is found in FLUENT by default, which is the k – ε equation where k is the turbulence kinetic energy and ε is the dissipation rate.

The absorption column meshing is prepared with height 6.55m and diameter of 0.1m. The meshing has a total of 104,800 quadrilateral cells. The meshing is then exported into FLUENT software from GAMBIT software. The appropriate FLUENT models are selected, UDFs are hooked to FLUENT and appropriate parameters are keyed into FLUENT software to run the simulation.

The absolute convergence criterion is set at 0.001 and the simulation is iterated until the solution converges. The results are then analyzed and justified. The results collected are then validated with a journal by Tontiwachwuthikul et al. (1992) with the journal title of 'CO_2 Absoprtion By NaOH, Monoethanolamine and 2-Amino-2-Methyl-1-Propanol Solutions in A Packed Column'. This is because the works of Tontiwachwuthikul et al. (1992) is exactly the same as the works of the author of the research. The works conducted by Tontiwachwuthikul et al. (1992) is experimental work while the works of the author of the research is simulation work.

4.1.2 Simulation Results based on FLUENT

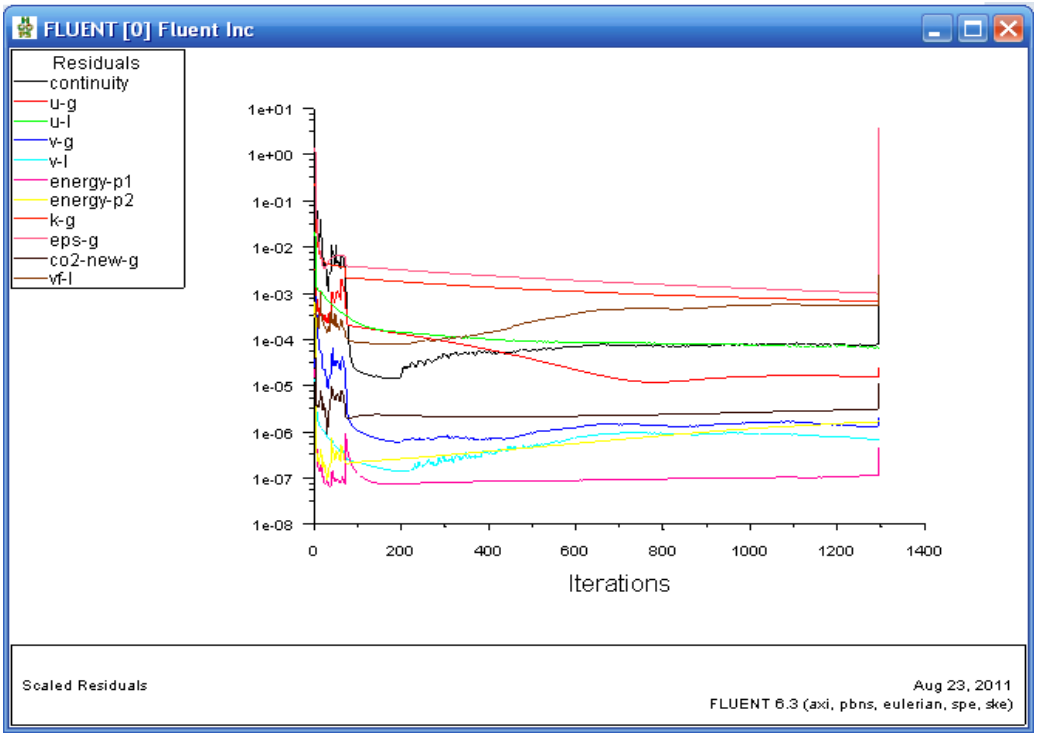

Figure 8: Iterations for Scaled Residuals until Convergence

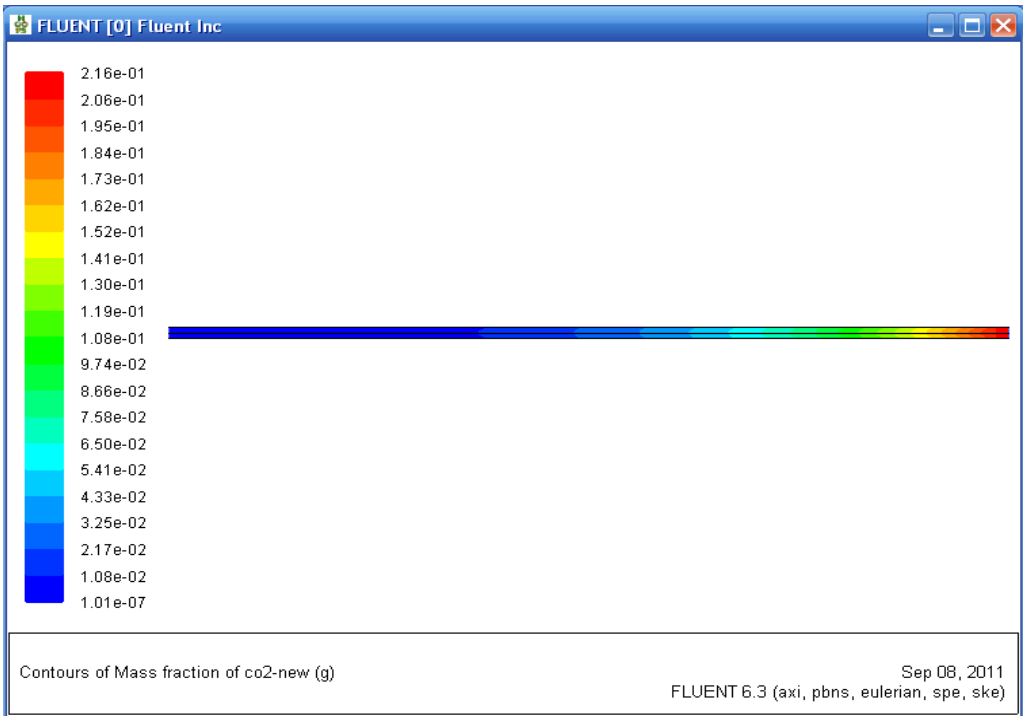

Figure 9: Mass Fraction of CO_2 Contour

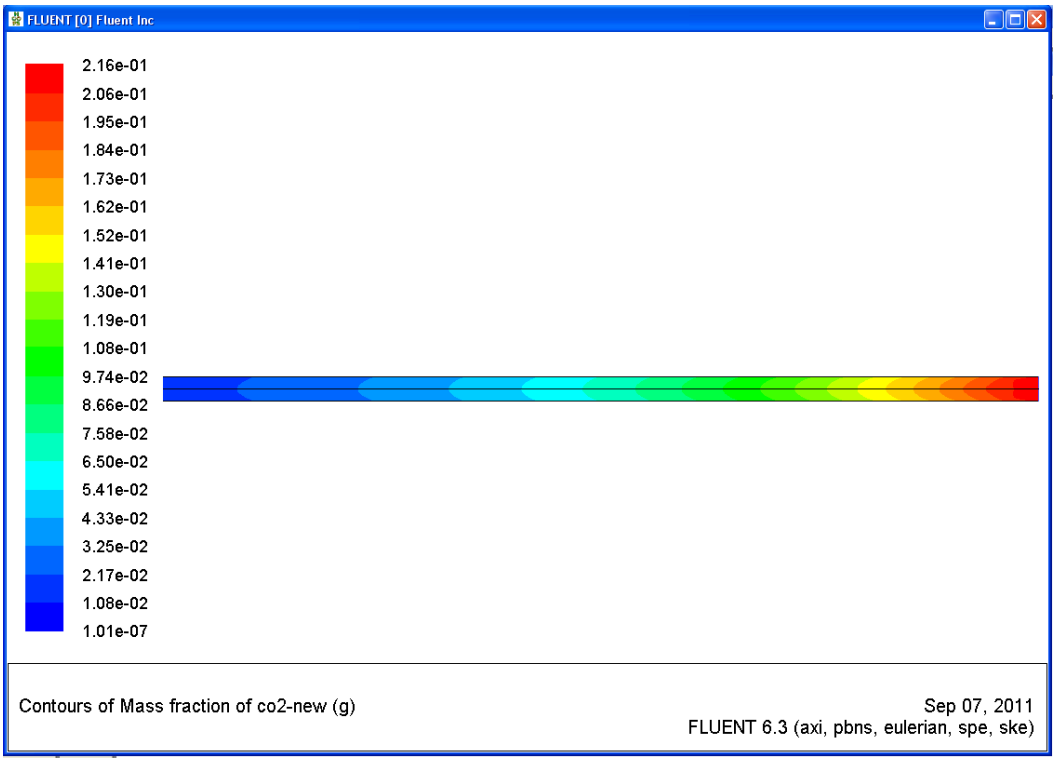

Figure 10: Mass Fraction of CO_2 Contour (zoom in)

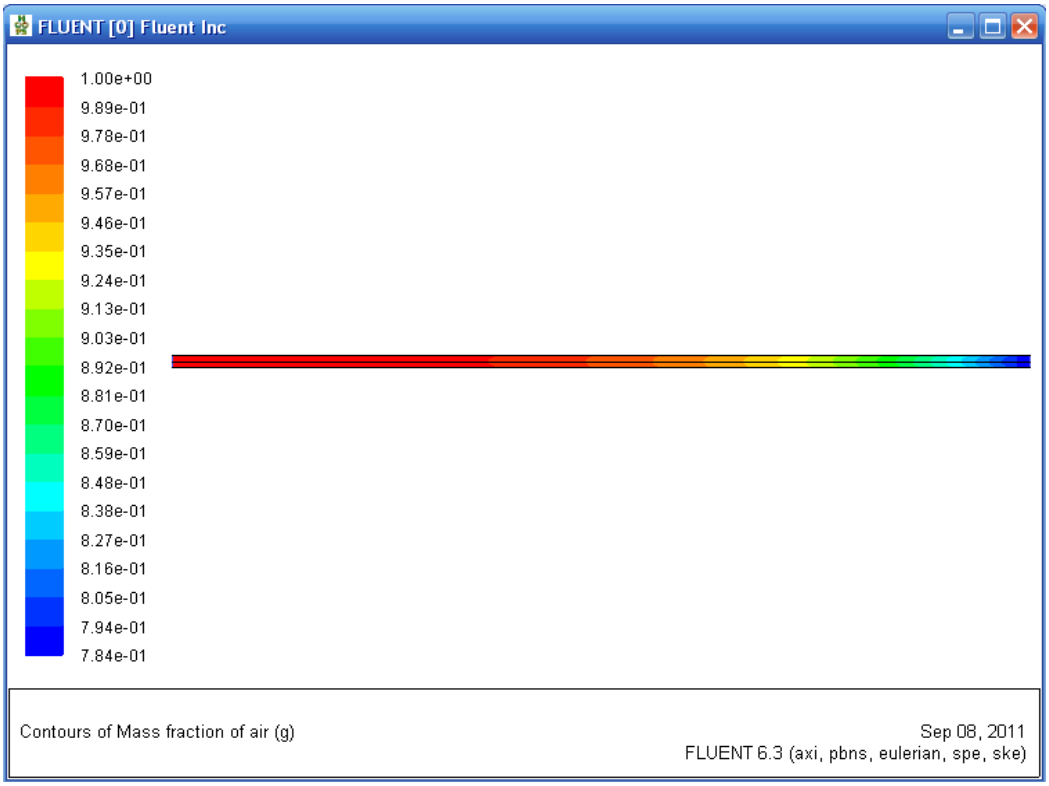

Figure 11: Mass Fraction of Air Contour

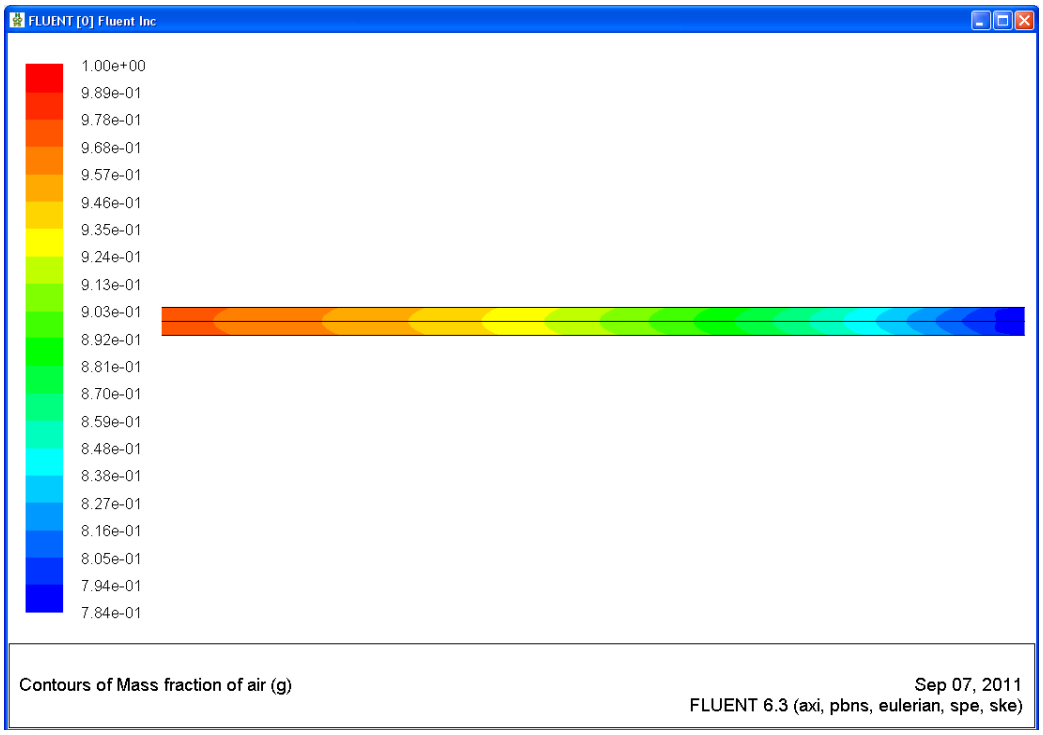

Figure 12: Mass Fraction of Air Contour (zoom in)

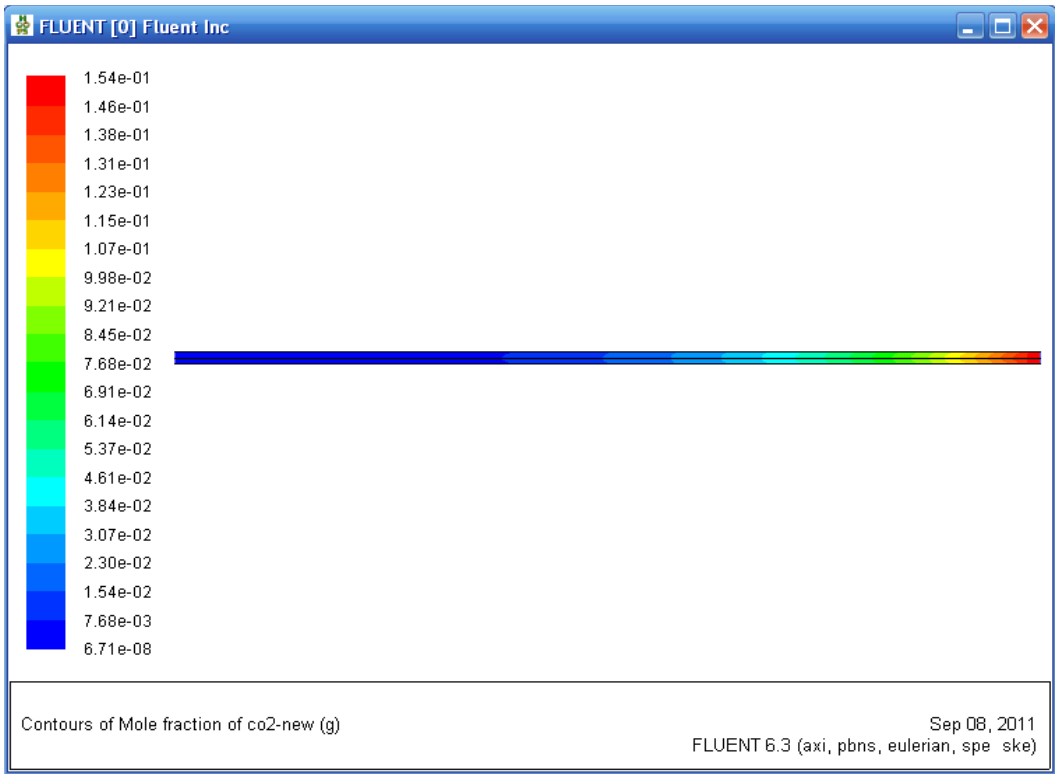

Figure 13: Mole Fraction of CO_2 Contour

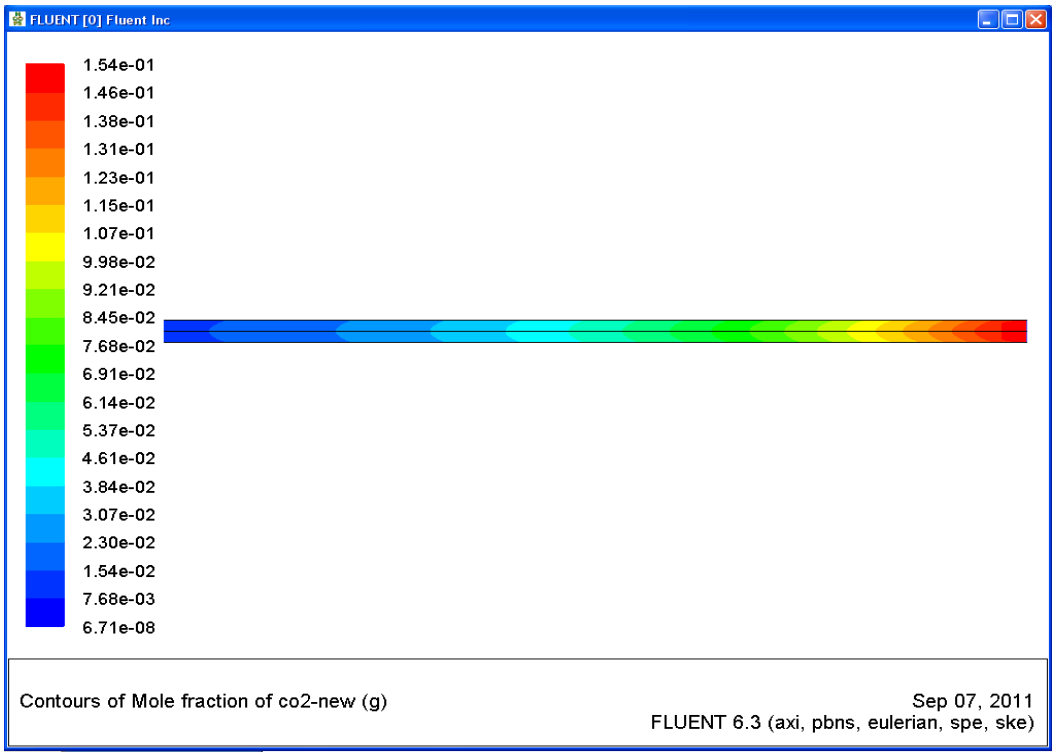

Figure 14: Mole Fraction of CO_2 Contour (zoom in)

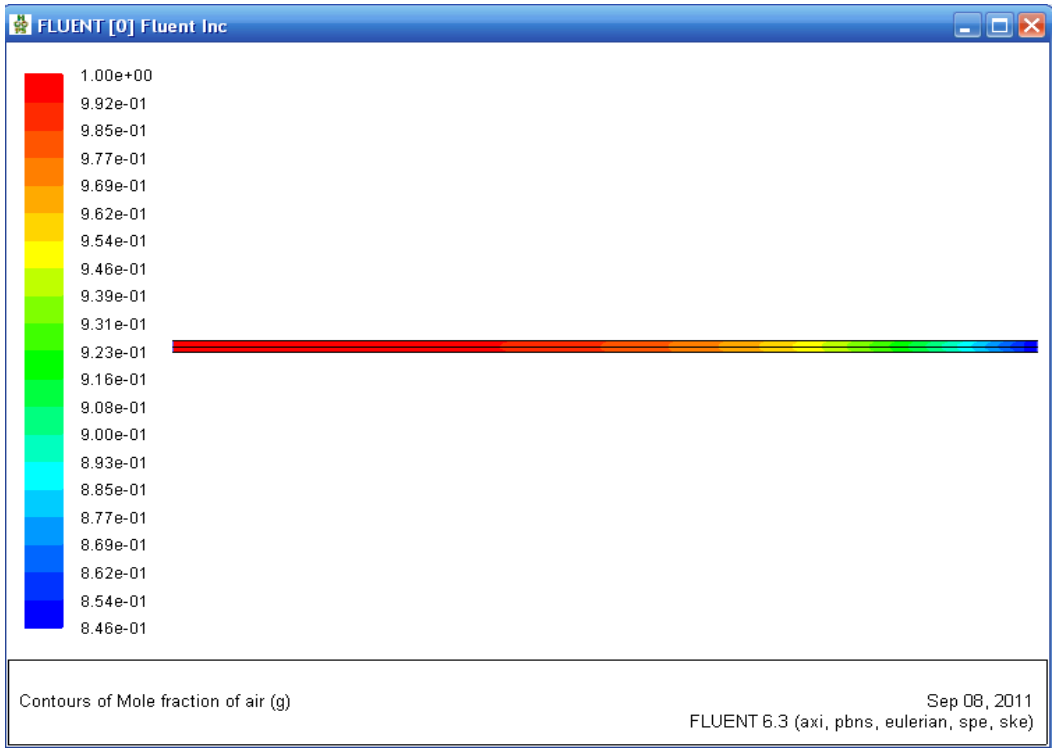

Figure 15: Mole Fraction of Air Contour

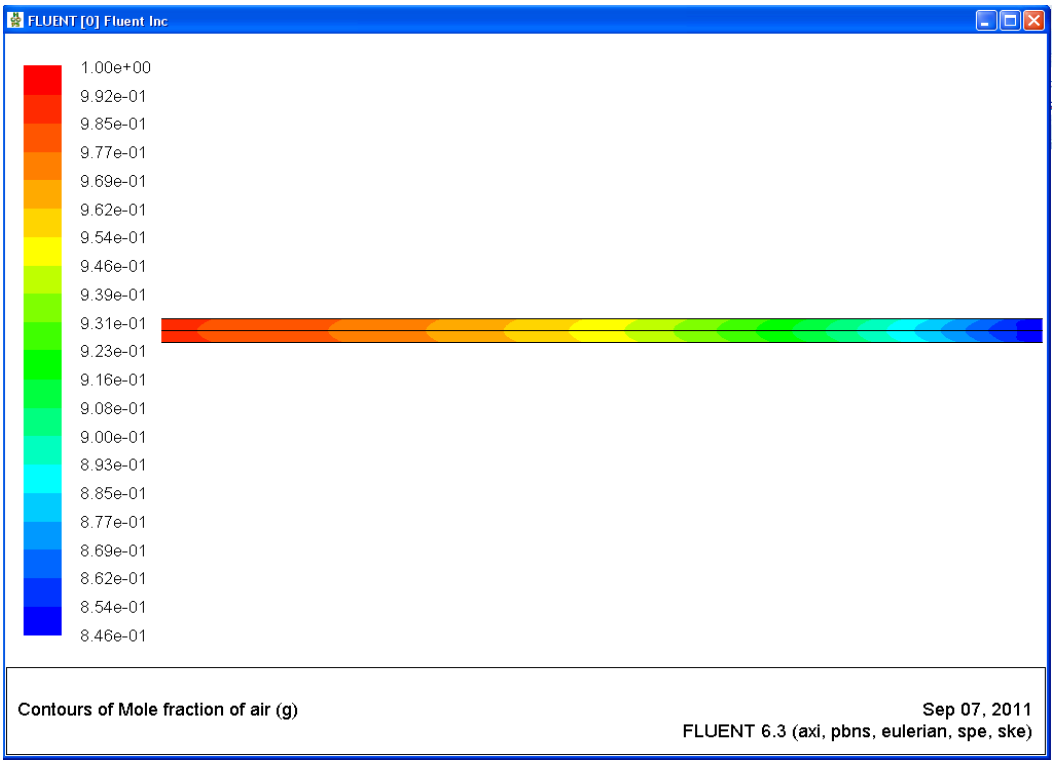

Figure 16: Mole Fraction of Air Contour (zoom in)

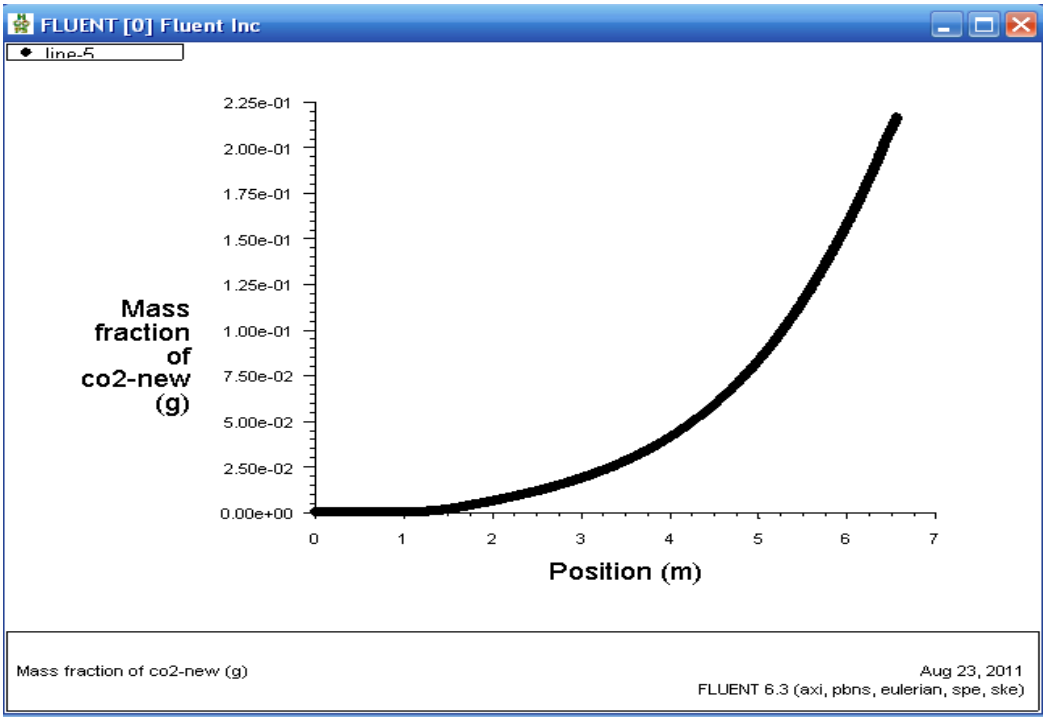

Figure 17: Mass Fraction of CO_2 across the Column

(Position 0m being the top of the column and 6.55m being the bottom of the column)

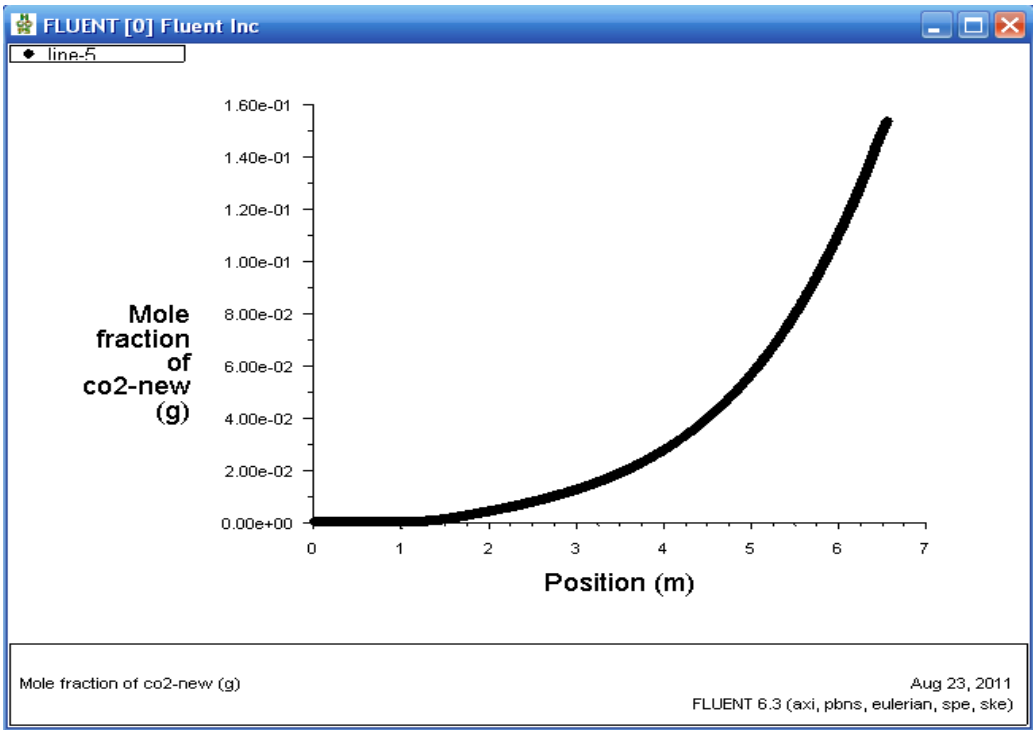

Figure 18: Mole Fraction of CO_2 across the Column

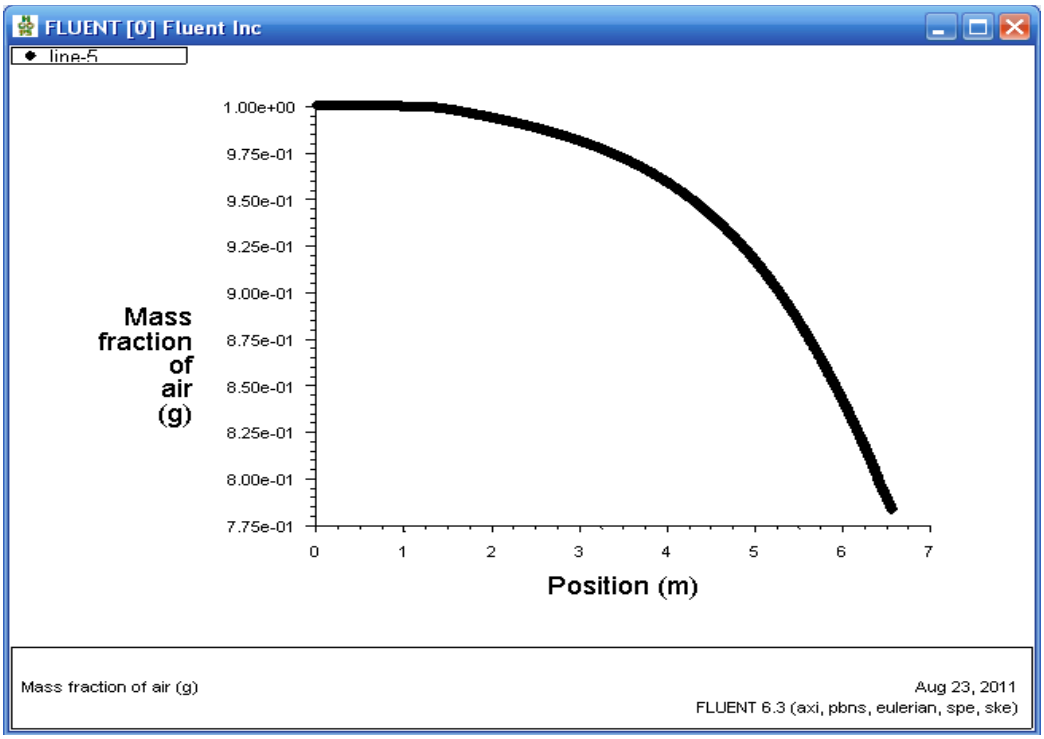

Figure 19: Mass Fraction of Air across the Column

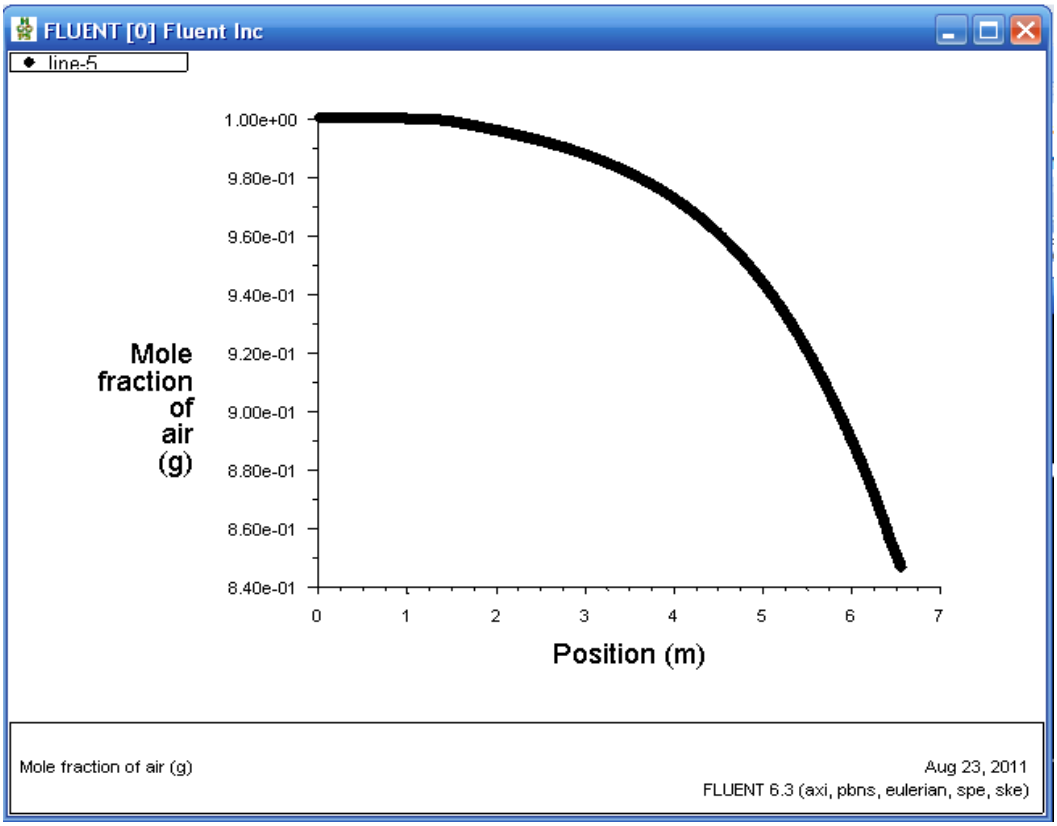

Figure 20: Mole Fraction of Air across the Column

4.1.3 Discussion

From Figure 8, the simulation is done and iterated until it reaches convergence. Figure 9 shows the mass fraction of CO_2 in the column whereas Figure 13 shows the mole fraction of CO_2 within the column. Figure 17 shows the mass fraction of CO_2 across the column. Figure 18 shows the mole fraction of CO_2 across the column. Meanwhile figure 19 and 20 shows the mass fraction and mole fraction of air across the column respectively.

Based on Figure 9 and 17, it can be observed that in Figure 17, the mass fraction of CO_2 in the column lessens as the gas flows to the top of the column. The inlet mass fraction of CO_2 in the gas phase is set to be at 0.2165. Due to this, as what can be observed in Figure 17, the mass fraction of air increases as the gas flows from the bottom of the column (x = 6.55m) to the top of the column (x = 0m).

This is because in the gas phase, there is a combination of both air and CO_2. The mass fraction of CO_2 is set at 0.2165 hence the mass fraction of air is 1 – 0.2165 which would be 0.7835. By the time the gas reaches to the top of the column, mass transfer between CO_2 and aqueous MEA solvent has been performed. The amount of CO_2 in the gas has completely transferred to the aqueous MEA solvent, thus leaving the mass fraction of CO_2 at top of the column to be 0, and the mass fraction of air to be 1.

The same explanation can be used to describe Figure 11 and 19, which is the mole fraction of air respectively in the column. Based on literature review, it is known that when mass transfer occurs, the CO_2 (solute) is transferred into aqueous MEA (solvent). So from the explanation above, it can be concluded that the mass transfer between CO_2 and aqueous MEA solvent has occurred successfully and the gas leaving the top of the column would be free from solutes (lean gas as per Figure 3).

The solvent entering the column was aqueous MEA solvent and now after mass transfer, the solvent exiting the bottom of the column would be rich with CO_2 solute where the CO_2 solute will completely be dissolved in the aqueous MEA solvent.

4.1.4 Justification of Research

As mentioned previously, the works of this research would be compared to the works of Tontiwachwuthikul et al. (1992) as both the research employ the same parameters and objective of research. Tontiwachwuthikul et al. (1992)'s work is experimental based meanwhile the author's work is simulation based. Below shows the results from Tontiwachwuthikul et al. (1992)'s work.

Run (#)	T13
Air flow (mol/m² s)	14.8
Liquid flow (m³/m² h)	13.5
MEA feed (kmol/m³)	2.00
Gas CO_2 concentration (%)@	
$z' = 0.00$ m	0.0
$z' = 1.05$ m	0.0
$z' = 2.15$ m	0.4
$z' = 3.25$ m	1.0
$z' = 4.35$ m	3.3
$z' = 5.45$ m	8.3
$z' = 6.55$ m	15.3
CO_2 removal (%)	100.0
CO_2 loading (mol CO_2/mol MEA)@	
$z' = 0.00$ m	0.000
$z' = 1.05$ m	(0.000)
$z' = 2.15$ m	(0.012)
$z' = 3.25$ m	0.025
$z' = 4.35$ m	0.078
$z' = 5.45$ m	0.200
$z' = 6.55$ m	0.362
Mass balance (%)	+ 2.36
Liquid temperature (°C)@	
$z' = 0.00$ m	19.0
$z' = 1.05$ m	19.0
$z' = 2.15$ m	19.5
$z' = 3.25$ m	20.0
$z' = 4.35$ m	23.0
$z' = 5.45$ m	29.0
$z' = 6.55$ m	34.0

Figure 21: Experimental Results from Journal

(Source: Tontiwachwuthikul et al., 1992)

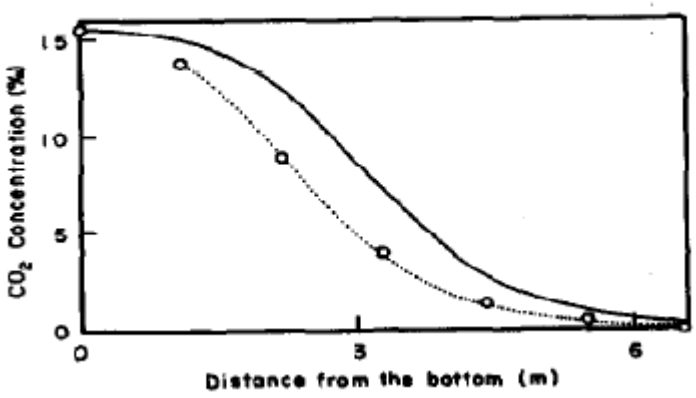

Figure 22: CO_2 Concentration (mol %) along the Column

(Source: Tontiwachwuthikul et al., 1992)

Since the author did research regarding the mass fraction of CO_2 in the column, the results will be compared with gas CO2 concentration (%) from Tontiwachwuthikul et al. (1992)'s work.

Gas CO_2 concentration (%)[a]	
$z' = 0.00$ m	0.0
$z' = 1.05$ m	0.0
$z' = 2.15$ m	0.4
$z' = 3.25$ m	1.0
$z' = 4.35$ m	3.3
$z' = 5.45$ m	8.3
$z' = 6.55$ m	15.3

Figure 23: Gas CO_2 Concentration (%) at Different Column Heights
(Source: Tontiwachwuthikul et al., 1992)

For comparison to be done, the mol % of CO2 concentration from Tontiwachwuthikul et al. (1992)'s work will be converted into mass fraction based on the formula below.

For example, at z = 6.55m, CO_2 concentration is 15.3 mol %, which is equivalent to 0.153 mol of CO_2.

$$\text{Mole} = \frac{\text{Mass}}{\text{Molecular Weight}}$$

The molecular weight of CO_2 = 44.00995 g/mol.
The molecular weight of air = 28.996 g/mol.
Mole fraction of CO_2 = 0.153
Mole fraction of air = 1 – 0.153
= 0.847

Total gas mass = (Mole fraction x Molecular Weight)$_{CO_2}$ + (Mole fraction x Molecular Weight)$_{Air}$

= (0.153 x 44.00995) + (0.847 x 28.996)
= 31.29313435g

Mass fraction of CO_2 at 6.55m = ((0.153 x 44.00995) / (31.29313435))

= 0.2165

The same calculation is repeated for the remaining values and the mass fraction value of CO_2 is tabulated in the table below.

Column Height (m)	**Mole % of CO_2**	**Mass Fraction of CO_2**
0	0.0	0
1.05	0.0	0
2.15	0.4	0.0056
3.25	1.0	0.0141
4.35	3.3	0.0464
5.45	8.3	0.1167
6.55	15.3	0.2165

Table 5: Mass Fraction of CO_2 from Journal

(Source: Tontiwachwuthikul et al., 1992)

Column Height (m)	**Mass Fraction of CO_2**
0	2.20×10^{-7}
1.05	1.65×10^{-4}
2.15	0.0080
3.25	0.0234
4.35	0.0537
5.45	0.1140
6.55	0.2165

Table 6: Mass Fraction of CO_2 from Simulation

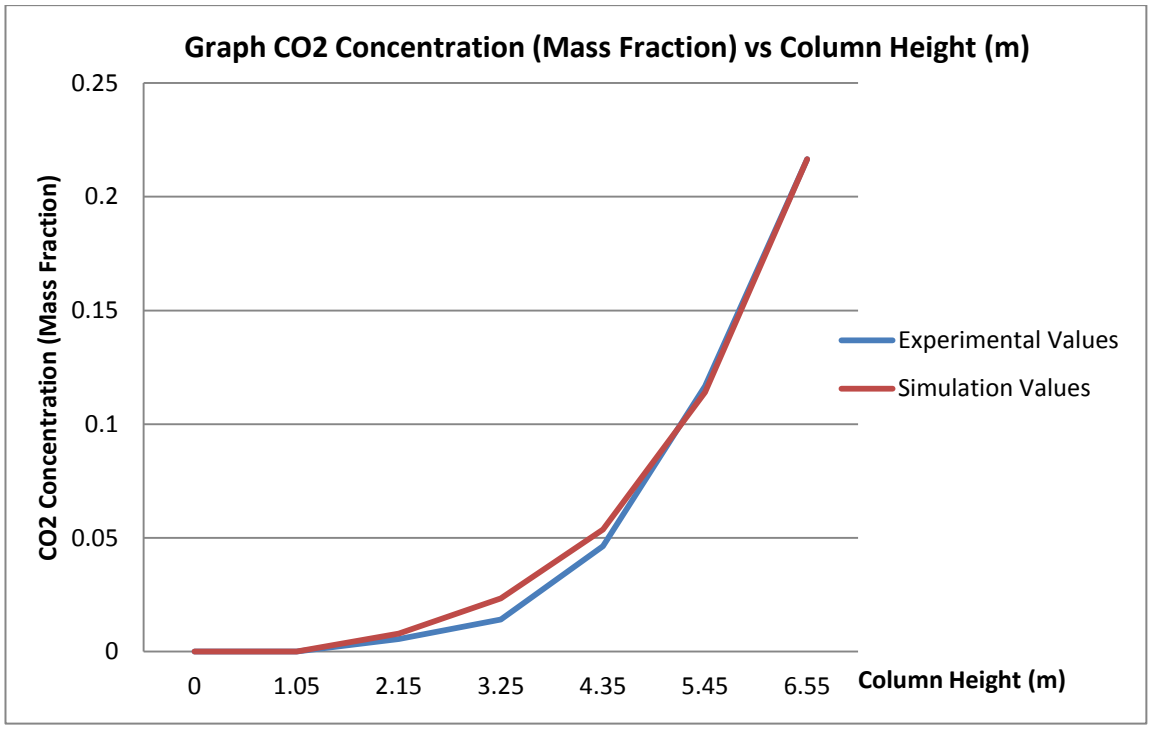

Figure 24: Comparison between Simulation Values and Experimental Values

Thus, from Figure 24 above, it can be concluded that the results are correct and are validated.

4.2 Results for Part II: To Determine the Effect of Different Column Length on Absorption Process

4.2.1 FLUENT Simulation

The simulation is then repeated exactly the same but for different column heights. In Part I, the column height used was 6.55m. For 6.55m column height, it can be observed that mass transfer between gas and liquid phase is completed once reaching the top of the column.

Thus it wouldn't be cost efficient to simulate the mass transfer for columns longer/higher than 6.55m as this would waste more cost into building higher columns for absorption purposes.

The author repeated the same simulation, using the same parameters for different column heights (i.e. 2.00m, 3.55m, 4.75m, and 5.75m) to determine the effect on different column heights on the absorption process.

4.2.2 Simulation Results based on FLUENT for 2.00m and Discussion

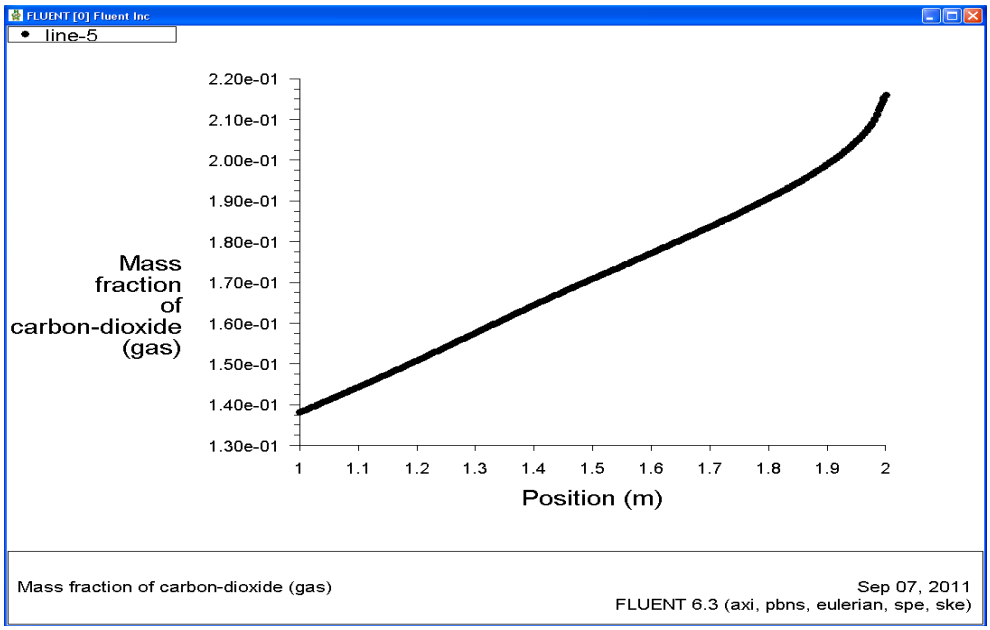

Figure 25: Mass Fraction of CO_2 across the Column for 2.00m

The mass fraction of contours for CO2 and air are attached in appendix iii.

For 2.00m column height, the simulation results are as shown in Figure 25. It can be observed that when the gas exits the top of the column, there is still a lot CO_2 left in the gas. This can be due to the fact that the absorption column is rather short thus limiting the chances for the gas phase and liquid phase to interact for absorption to happen.

The amount of CO_2 in the gas phase after exiting the column as extracted from FLUENT is around 0.137, which is very large. For column height of 6.55m, absorption process takes place and is completed when the gas exits the column. Comparing the results for both column heights, this shows that the column height of 2.00m is not sufficient for absorption process to complete entirely.

4.2.3 Simulation Results based on FLUENT for 3.55m and Discussion

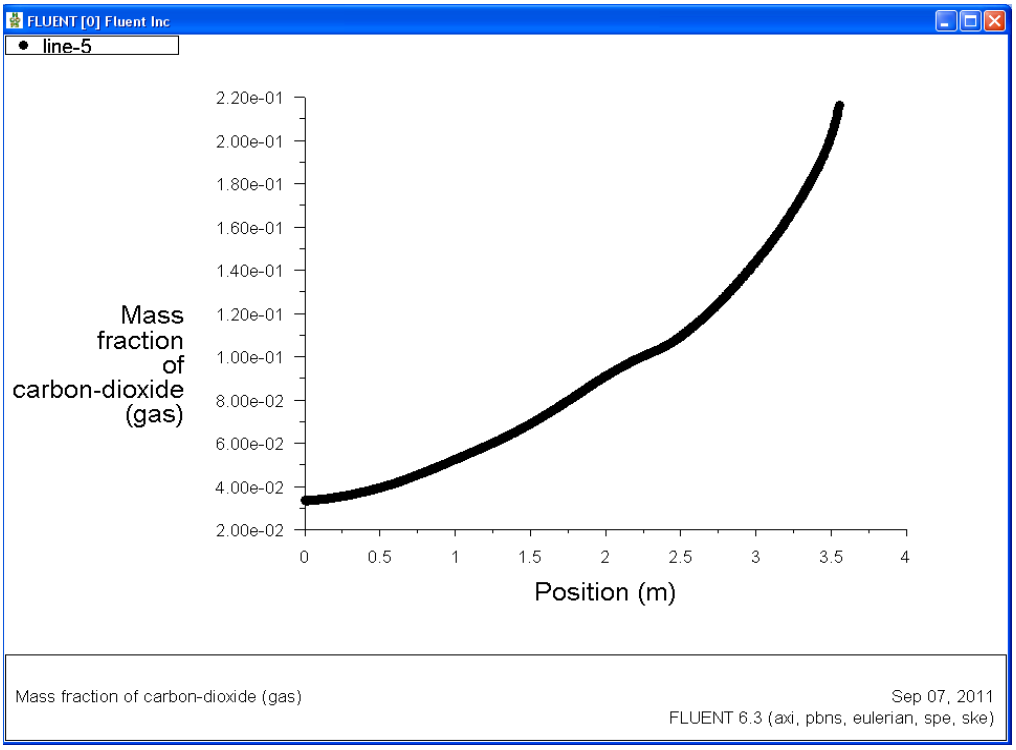

Figure 26: Mass Fraction of CO_2 across the Column for 3.55m

The mass fraction of contours for CO2 and air are attached in appendix iii.

As can be observed from Figure 26, the mass transfer between CO_2 solute and the aqueous MEA solvent is not completed. By the top of the column (0m), there is still some CO_2 left in the gas phase. From the FLUENT software, at the top of the column (0m), the amount of CO_2 left in the gas phase is still around 0.035.

As compared to column height of 2.00m, the amount of solute left for column height of 3.55m is smaller but nevertheless still insufficient. Absorption takes place but is not completed totally. Thus it can be concluded that this length of column is not suitable for the absorption process between CO_2 and aqueous MEA solvent because the amount of CO_2 solute left after exiting the column is still considered fairly large.

4.2.4 Simulation Results based on FLUENT for 4.75m and Discussion

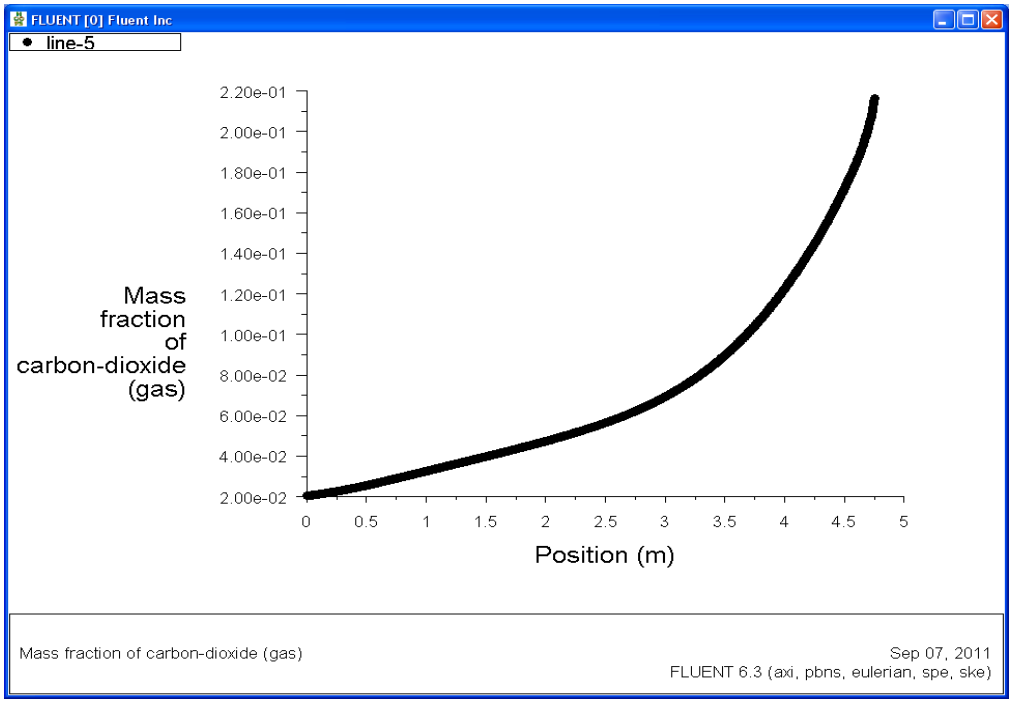

Figure 27: Mass Fraction of CO_2 across the Column for 4.75m

The mass fraction of contours for CO2 and air are attached in appendix iii.

From Figure 27, it can be observed that the curve for the X-Y Plot is now smoother, approaching the X-Y Plot curve for column height of 6.55m. But at this column height, although absorption process takes place, but the absorption process between CO_2 solute and MEA solvent did not complete entirely as well. By the top of the column, there is still some CO_2 left in the gas phase, which is roughly around 0.0202.

Once again, it can be concluded that this length of column is still not suitable for complete absorption process between CO_2 and aqueous MEA solvent because the there is still CO_2 left in the gas phase.

4.2.5 Simulation Results based on FLUENT for 5.75m and Discussion

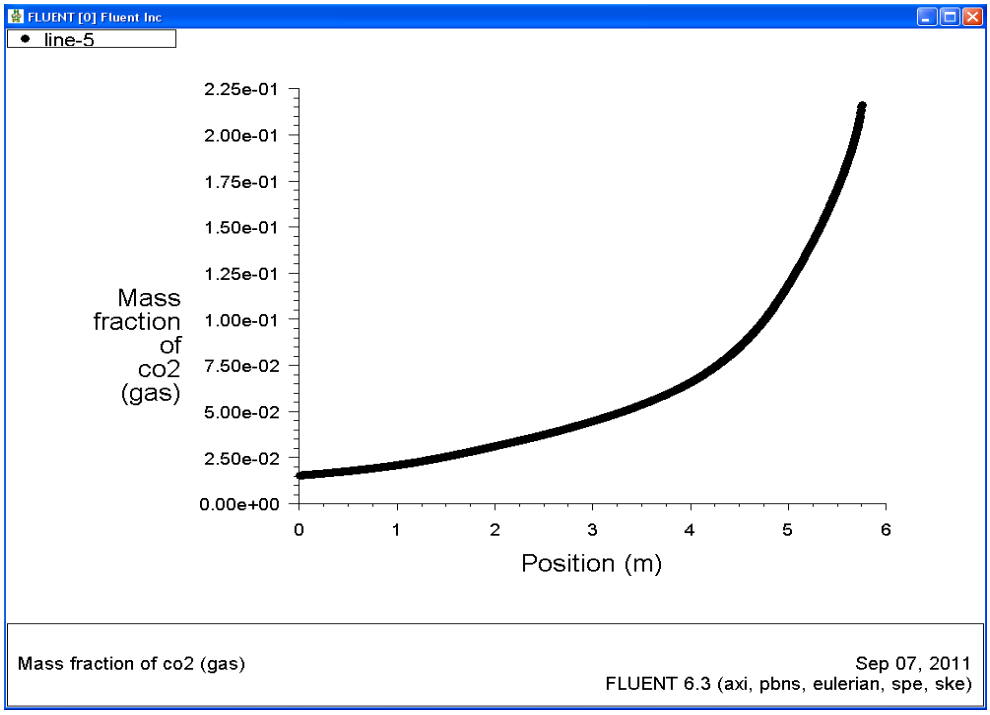

Figure 28: Mass Fraction of CO_2 across the Column for 5.75m

The mass fraction of contours for CO2 and air are attached in appendix iii.

The simulation is then repeated for column height of 5.75m. After the iteration finishes and the solution converges, it is still observed that by the time the gas phase exits the top of the column, there is still traces of CO_2 solute within the gas. This means that the mass transfer between CO_2 solute and aqueous MEA solvent did not completely finish by the time the gas reaches the top.

From FLUENT software, the amount of CO_2 left in the gas phase at column height of 0m is 0.0151. This values show that there is still a considerable amount of CO_2 left in the gas phase which has not been absorbed by the aqueous MEA solvent.

Thus the author can conclude that different column heights can give different effects to the CO_2 absorption into aqueous MEA solvent. The appropriate column height is still 6.55m for complete mass transfer process.

4.2.6 Justification of Research

The works done for this part can be justified with the trend obtained from Tontiwachwuthikul et al. (1992)'s research. The same graph of Absorber Height vs CO_2 Concentration Left is plotted from the results obtained from simulation. The trend of both graphs are the same, thus the results are justified. As can be observed from both figures, the higher/taller the absorber is, the more CO2 is absorbed, thus the removal of CO2 solute from gas phase is more complete due to enough contact between gas and liquid phase for mass transfer.

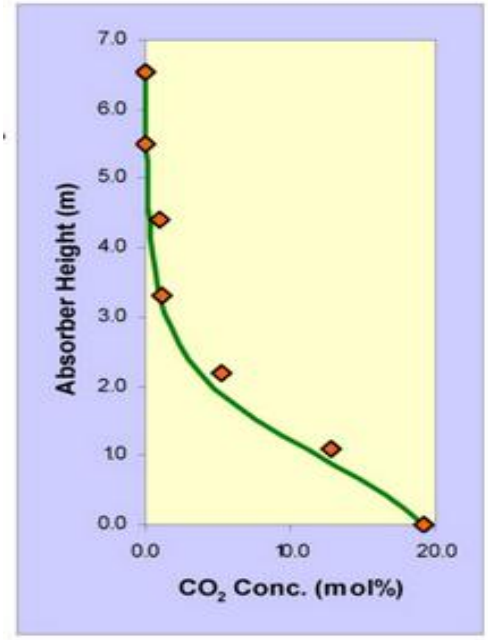

Figure 29: Effect of Absorber Height on Removal of CO_2 Concentration (Source: Tontiwachwuthikul et al. (1992))

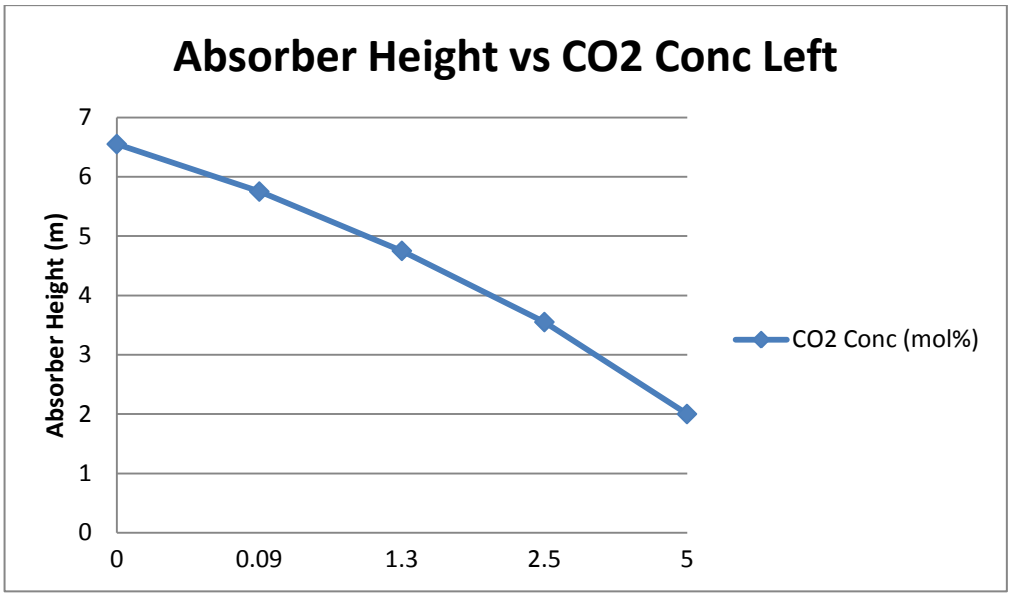

Figure 30: Effect of Absorber Height on Removal of CO_2 Concentration based on Simulation Results

4.3 Results for Part III: To Determine the Effect of Different Gas Velocity on Absorption Process

4.3.1 FLUENT Simulation

The simulation is once again conducted for different gas velocities to determine the effect of gas velocities on the absorption process between the gas and liquid phase. Based on Tontiwachwuthikul et al.'s work (1992), Tontiwachwuthikul et al. proposed a range of different gas velocities that can be used to determine the effect on absorption process: Superficial Gas Flow Rate = 11.1 to 14.8mol/m^3s.

The flooding point is calculated to determine the values of gas velocities to use. The Generalized Pressure Drop Correlation (GPDC) chart extracted from Kister's Distillation Design (Kister, 1992) is used to aid in flooding point calculation. The GPDC chart and calculations for flooding point can be found in appendix ii.

Flooding point calculated = 1.8413 kg/m^2s. Thus the author will be using 3 different gas velocities in Part III of the research, which would be G = 0.347 kg/m^3s, G = 0.519 kg/m^3s and G = 1.30 kg/m^3s. The effect of these different gas velocities will be discussed in the following section.

4.3.2 Simulation Results for G = 0.347 kg/m^{3}s and Discussion

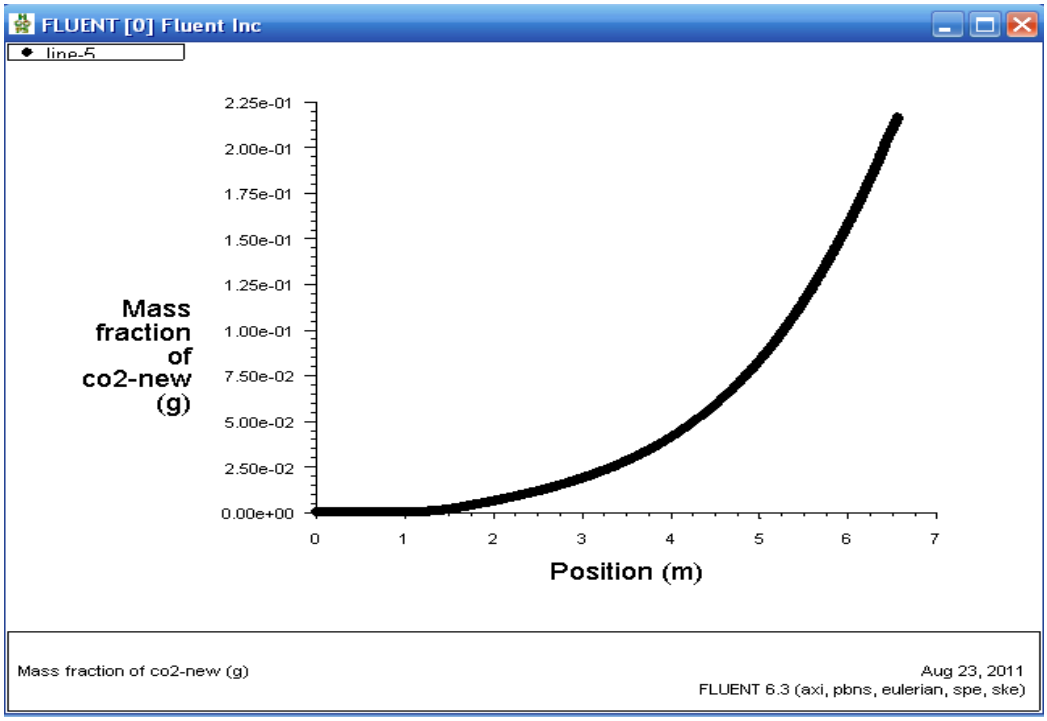

Figure 31: Mass Fraction of CO_2 across the Column for G = 0.347 kg/m^{3}s

The mass fraction of contours for CO2 and air are attached in appendix iii.

For this section, the value of gas velocity introduced into the column is 0.347 kg/m^{3}s, whereby the gas velocity is lower than the initial gas velocity introduced in Part I. When the gas velocity introduced into the column is low, this enables the gas phase to slowly flow up the column, thus maximizing contact with the liquid phase flowing down the column.

When this happens, the residence time for both phases in the column will tend to be higher, thus providing ample contact for both phases for absorption to happen. Absorption process happens between CO_2 solute and aqueous MEA solvent and due to the fact that there is high residence time in the column, the absorption rate between gas phase and liquid phase would be high.

Based on Figure 31, absorption process happens and it fully completed as gas flows upwards and liquid flows downwards along the column. From FLUENT software,

the amount of CO_2 left in the gas phase is obtained to be 0 at the end of the column. Mass transfer completes at column height of 1.15m.

4.3.3 Simulation Results for G = 0.519 kg/m^{3}s and Discussion

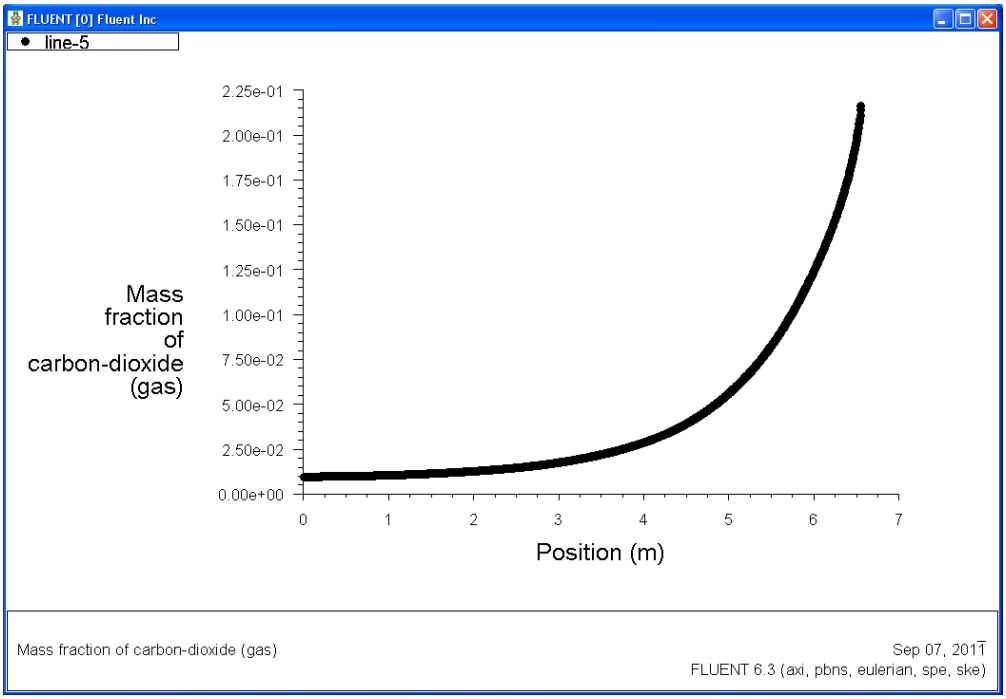

Figure 32: Mass Fraction of CO_2 across the Column for G = 0.519 kg/m^{3}s

The mass fraction of contours for CO2 and air are attached in appendix iii.

As per Figure 32, it can be seen that at the top of the column where the gas phase exits, there is still a considerable amount of CO_2 solute left within the gas phase. The amount of CO2 left in the gas phase is around 0.015 as extracted from the FLUENT software. This means that although absorption process happens, it did not finish completely.

This could be due to the fact that when higher gas velocity is introduced into the column, as the gas flows faster throughout the column with constant liquid flow rate, there is lesser residence time between the gas phase and liquid phase in the column, hence lowering the contact between both gas and liquid phase. When this happens, absorption process happens but is not as effective as compared to low gas velocities. This means that there are lesser and more limited contact between both phases, hence limiting the absorption process between aqueous MEA solvent and CO_2 solute.

This can be concluded and justified from Figure 32 whereby there is still a considerable amount of CO_2 solute left in the gas phase after exiting the top of the column.

4.3.4 Simulation Results for G = 1.3 kg/m^{3}s and Discussion

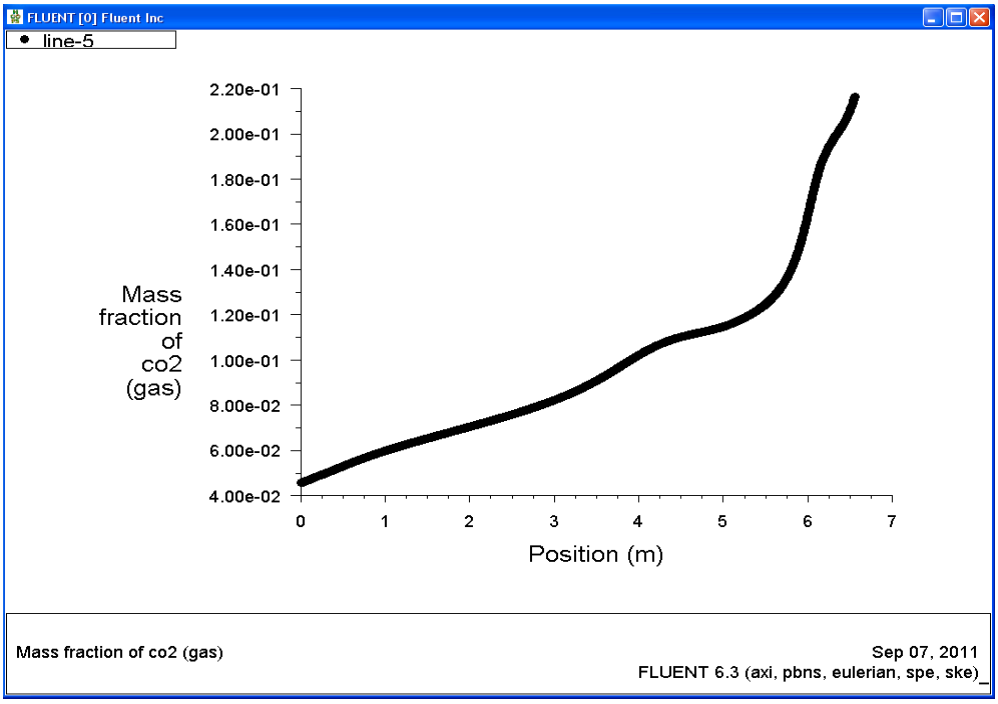

Figure 33: Mass Fraction of CO_2 across the Column for G = 1.3 kg/m^{3}s

The mass fraction of contours for CO2 and air are attached in appendix iii.

The curve of the mass fraction of CO_2 across the column from the simulation results is not smooth as compared to the curve results obtained from Figure 31 and 32. This is because the gas velocity used for this part is 1.3 kg/m^{3}s, which is above the flooding point limitation of 1.2889 kg/m^{2}s. In the industry, it is practiced that the maximum gas velocity that can be channeled into an absorption column is 70% of the flooding point. This is to make sure that flooding doesn't occur within the column.

The flooding point as calculated using the GPDC chart is 1.8413 kg/m^{2}s. Thus, due to the fact that the gas velocity for this part is above the flooding point limitation, this

might be the reason why the curve is not smooth despite absorption between CO_2 solute and aqueous MEA solvent happens.

4.3.5 Justification of Research

The results for this part can be justified with the results done by Faiz et al. (2011). It can be seen that there's a trend between both graphs, whereby the higher the gas flow rate is, the percentage of removal of CO_2 is lesser and vice versa. The results obtained from FLUENT software indicate the same, as shown in Figure 35.

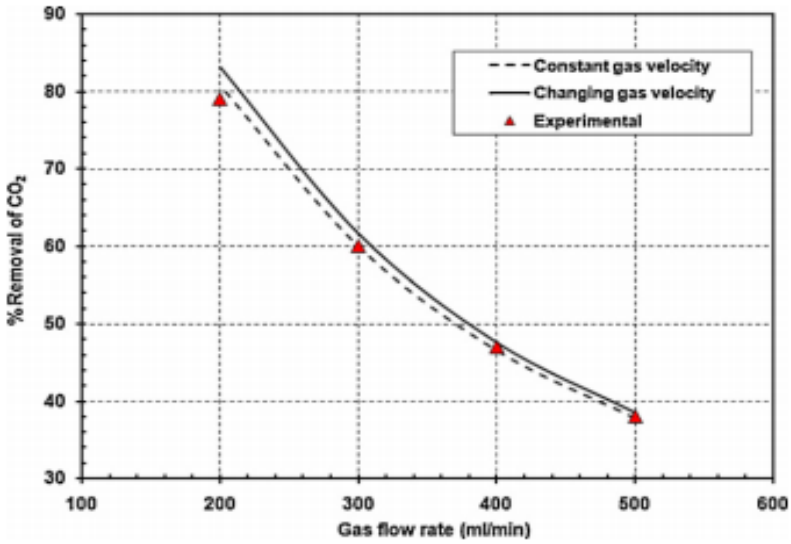

Figure 34: Graph of % Removal of CO2 vs Gas Flow Rate (Source: Faiz et al. (2011))

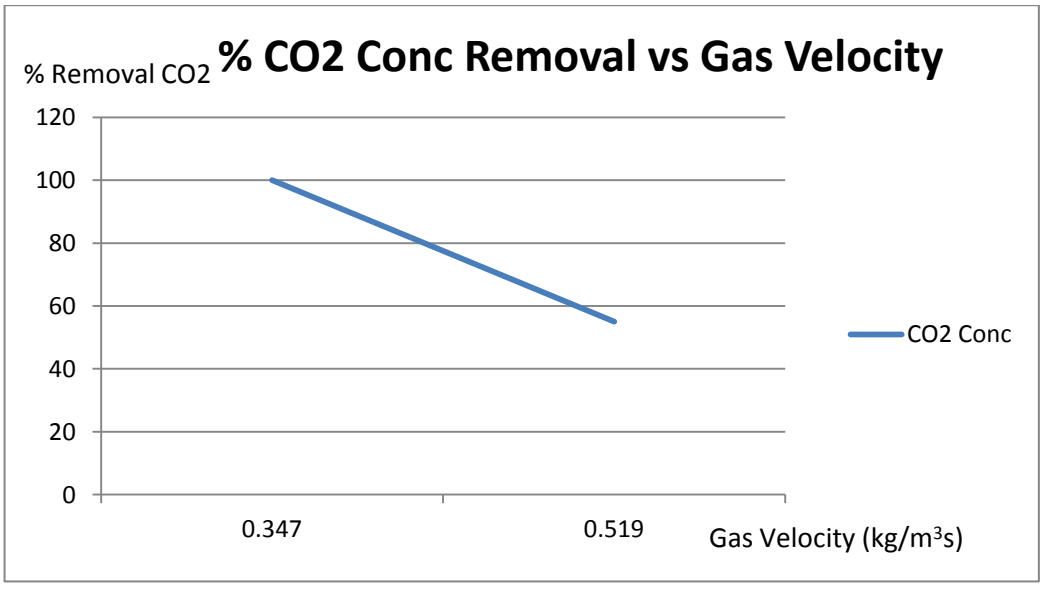

Figure 35: Graph of % Removal of CO2 vs Gas Flow Rate from Simulation

4.4 Results for Part IV: Grid Sensitivity Analysis

4.4.1 FLUENT Simulation

The simulation is repeated various times in order to perform grid sensitivity analysis. Grid sensitivity analysis is performed because the number of grids to be used in a simulation has considerable effect on the numerical results. This means that different meshing grids may produce different simulation results. Simulation is repeated to determine the best grid used for meshing.

4.4.2 Grid Sensitivity Analysis for Axial Direction

For the default mesh criteria as proposed by Liu et al. (2006), the number of nodes proposed is 1310 (interval counts) with successive ratio of 1. The velocity magnitude of gas phase from the simulation results was observed.

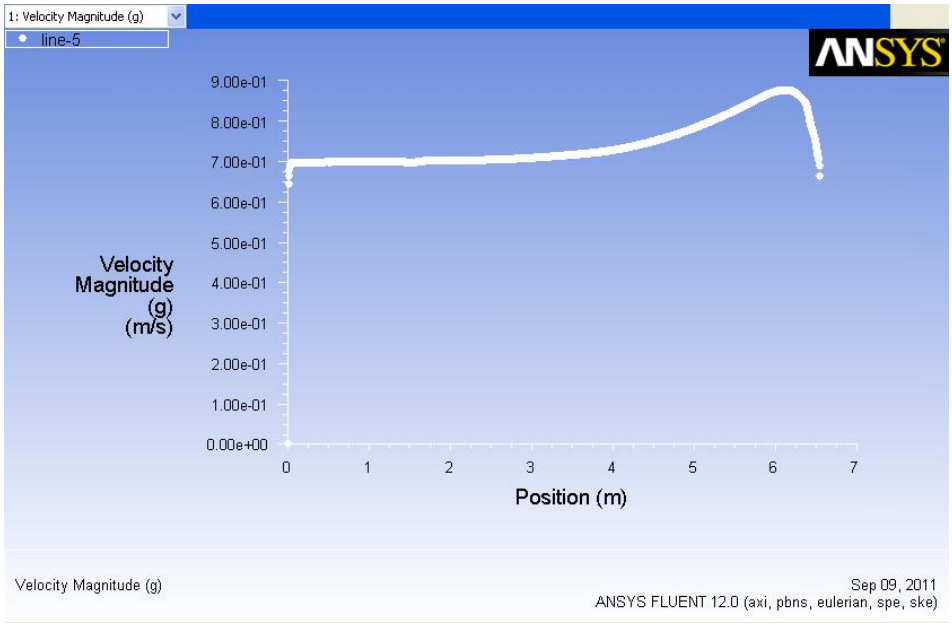

Figure 36: Velocity Magnitude of Gas Phase

The simulation was repeated for different interval counts to observe the effect on the results. The results were compared in terms of gas phase velocity magnitude. It was found that interval counts of 1304 nodes until 1385 nodes yields the same velocity magnitude results as per 1310 nodes. The X and Y values for each simulation was obtained from FLUENT software and a graph was plotted.

This means that interval counts from 1304 nodes until 1385 nodes yield the same results, but however, there is no doubt that the numerical accuracy could be further improved by more precise simulation.

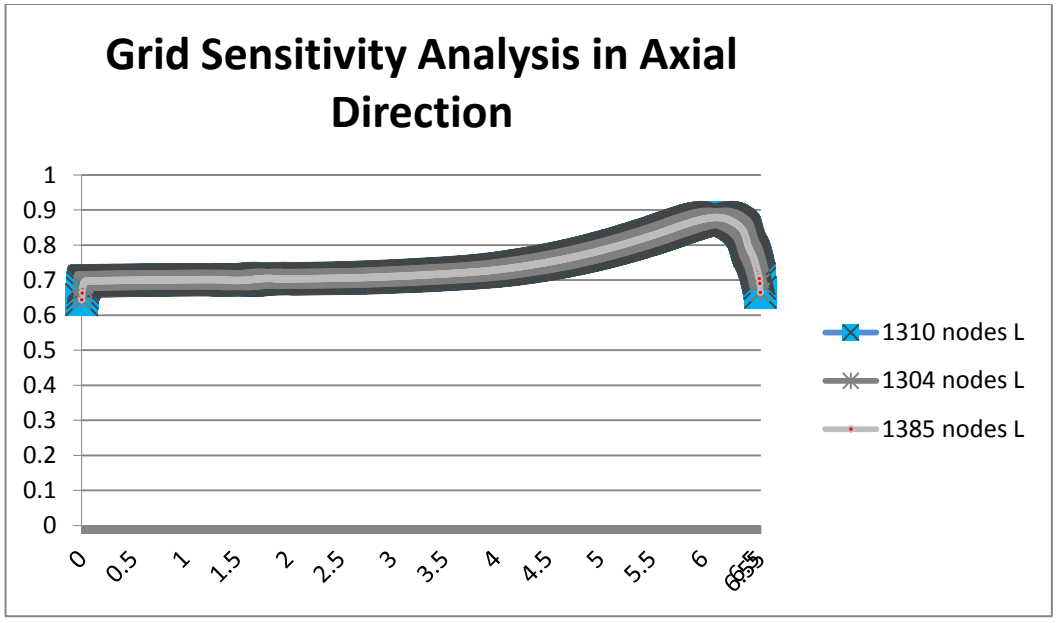

Figure 37: Grid Sensitivity Analysis in Axial Direction

4.4.3 Grid Sensitivity Analysis for Radial Direction

For the default mesh criteria as proposed by Liu et al. (2006), the number of nodes proposed is 80 with exponent ratio of 0.29 (non uniformly distributed). The velocity magnitude of gas phase from the simulation results was observed.

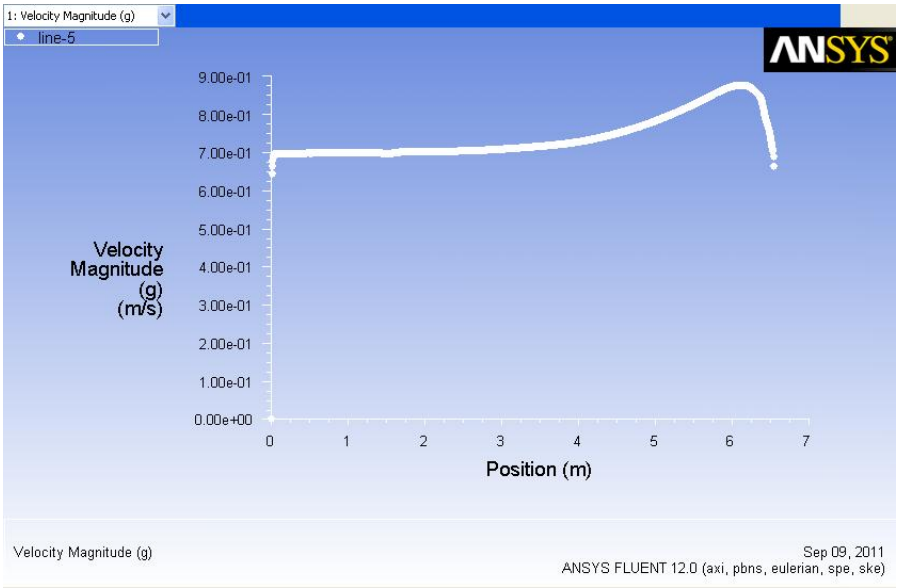

Figure 38: Velocity Magnitude of Gas Phase

The simulation was repeated for different interval counts to observe the effect on the results. The results were compared in terms of gas phase velocity magnitude. It was found that interval counts of 74 nodes until 225 nodes yields the same velocity magnitude results as per 80 nodes. The X and Y values for each simulation was obtained from FLUENT software and a graph was plotted.

This means that interval counts from 74 nodes until 225 nodes yield the same results, but however, there is no doubt that the numerical accuracy could be further improved by more precise simulation.

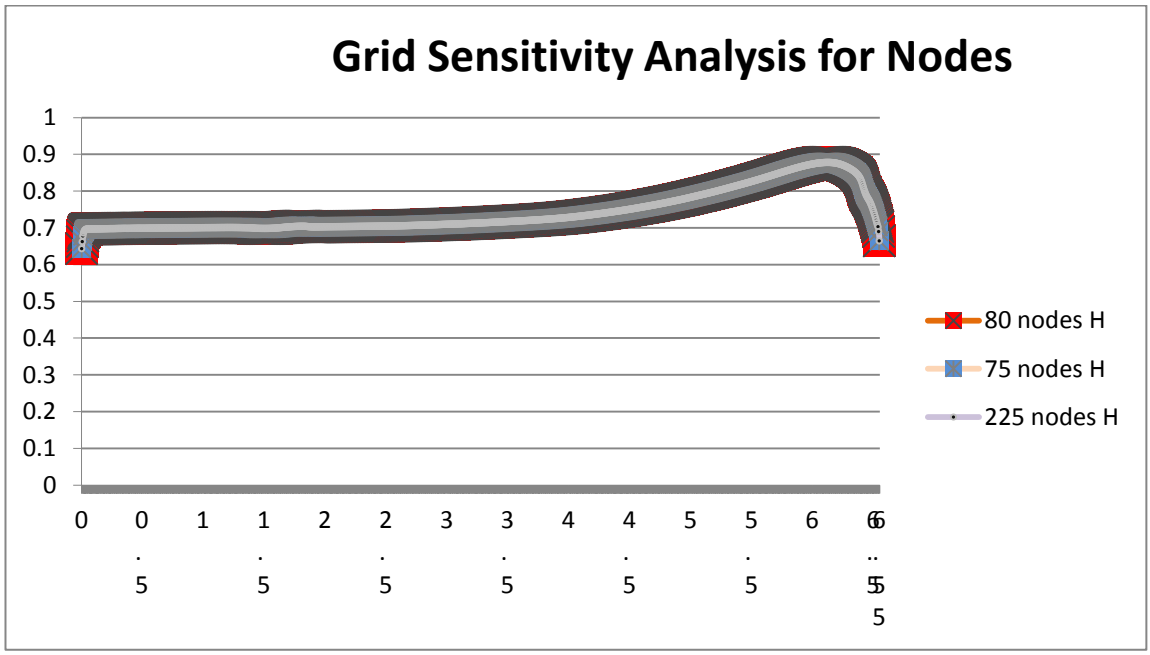

Figure 39: Grid Sensitivity Analysis in Radial Direction

CHAPTER 5
CONCLUSIONS AND RECOMMENDATIONS

In conclusion, it is proven and justified that absorption process can take place between CO_2 solute in gas phase and aqueous MEA solvent. Based on the first part of the research results, it is concluded that the amount of CO_2 solute in gas phase is successfully absorbed into the aqueous MEA solvent. This means that the mass transfer that takes place is successful. The validation of the research data with Tontiwachwutikul et al. (1992)'s work proves that the results are in satisfactory agreement.

For the second part of the research, it is shown that different column heights will affect the absorption process. This is because if the column height is shorter, the interaction between the gas and liquid phase will be limited and minimized. The interaction between gas and liquid phase is higher for longer columns as there are more contact area. Thus it is proven that different column heights will affect the mass transfer rate for CO_2 solute into aqueous MEA solvent. The trend of results was compared to Tontiwachwutikul et al. (1992)'s work.

For the third part, it is simulated that when the gas velocity is high, the residence time between both phases is low, limiting the contact between gas and liquid phase, thus lowering absorption process. Meanwhile for low gas velocity, from the simulation results, it can be seen that mass transfer between CO_2 solute and aqueous MEA solvent takes place completely. This is because there is higher residence time in the column, thus maximizing contact between gas and liquid phase. Due to this, absorption process can take place and is fully completed. The trend of results was compared to Faiz et al. (1992)'s work.

For the fourth part, the simulation was repeated for various interval counts and is observed that nodes from 75 to 225 are applicable for radial direction and nodes from 1304 to 1385 are applicable for axial direction. The numerical accuracy could be further improved by precise simulation using large number of grid points.